Highlights

Sources of marine debris for Seychelles and other remote islands in the western Indian Ocean

Vogt-Vincent, N.S., Burt, A.J., Kaplan, D., Mitarai, S., Turnbull, L.A., Johnson, H.L.

- We use Lagrangian trajectory analysis to quantify sources of marine debris for Seychelles and other remote islands in the western Indian Ocean.
- Most terrestrial debris beaching at Seychelles comes from Indonesia, with contributions from India, Sri Lanka, Tanzania, Comoros, and Seychelles itself.
- Seychelles is at very high risk from debris of marine origin from fisheries and shipping lanes.
- Debris accumulation rates across Seychelles are likely strongly seasonal, and possibly amplified during positive Indian Ocean Dipole and El Niño phases.

Sources of marine debris for Seychelles and other remote islands in the western Indian Ocean

Vogt-Vincent, N.S.[a], Burt, A.J.[b], Kaplan, D.[c,d], Mitarai, S.[e], Turnbull, L.A.[b], Johnson, H.L.[a]

[a]*Department of Earth Sciences, South Parks Road, University of Oxford, Oxford, UK*
[b]*Department of Plant Sciences, South Parks Road, University of Oxford, Oxford, UK*
[c]*MARBEC, Univ Montpellier, CNRS, Ifremer, IRD, Sète, France*
[d]*Institut de Recherche pour le Développement (IRD), MARBEC, av. Jean Monnet, CS 30171, Sète, France*
[e]*Marine Biophysics Unit, Okinawa Institute of Science and Technology Graduate University, Okinawa, Japan*

Abstract

Vast quantities of marine debris have beached at remote islands in the western Indian Ocean such as Seychelles, but little is known about where this debris comes from. To identify these sources and temporal patterns in accumulation rate, we carried out global Lagrangian particle tracking experiments incorporating surface currents, waves, and variable windage, beaching, and sinking rates, taking into account both terrestrial (coastal populations and rivers) and marine (fisheries and shipping) sources of debris. Our results show that, whilst low-buoyancy terrestrial debris may originate from the western Indian Ocean (principally Tanzania, Comoros, and Seychelles), most terrestrial debris beaching at remote western Indian Ocean islands drifts from the eastern and northern Indian Ocean, primarily Indonesia and, to a lesser extent, India and Sri Lanka. Purse-seine fragments beaching at Seychelles are likely associated with fishing activity in the western Indian Ocean, but longline fragments may also be swept from the southeastern Indian Ocean. The entire of Seychelles is at very high risk from waste discarded from shipping routes transiting the Indian Ocean, and comparison with observations suggests that many bottles washing up on beaches may indeed originate from these routes. Our analyses indicate that marine debris accumulation at Seychelles (and the Outer Islands in particular) is likely to be strongly seasonal, peaking during February-April, and this pattern is driven by local monsoonal winds. This seasonal cycle may be amplified during positive Indian Ocean Dipole phases and El-Niño events. These results underline the vulnerability of small island developing states to marine plastic pollution, and are a crucial first step towards improved management of the issue. The Lagrangian trajectories used in this study are available for download, and our analyses can be rerun under different parameters using the associated scripts.

Keywords: Marine debris, Indian Ocean, Seychelles, Plastic, Monsoon, Lagrangian

---

1. Introduction

Marine plastic pollution is a significant environmental threat, both for marine ecosystems (Gall and Thompson, 2015), and the communities that depend on the ocean for sustenance, tourism, and other social and economic activities (Thompson et al., 2009; Werner et al., 2016). Only a small proportion of plastic thought to have entered the marine environment remains floating at the ocean surface (Cózar et al., 2014), with the vast majority sinking to deep sea sediments (Woodall et al., 2014) or beaching on coasts (Onink et al., 2021). Beached marine debris in particular is of great concern; coastal environments are highly productive and biodiverse so the accumulation of debris on coasts can be damaging to both marine and terrestrial organisms (e.g. Nelms et al., 2016; Bergmann et al., 2017), and is associated with significant economic costs (Newman et al., 2015). On some coastlines, much of the accumulated debris may be of local origin (e.g. Martinez-Ribes et al., 2007; Turrell, 2020). Elsewhere, however, particularly in the case of remote islands with minimal or no local population, most debris accumulating on the coast may have been transported over great distances by ocean currents, winds, and waves prior to beaching (van Sebille et al., 2020). These islands, many of which belong to small island developing states, are faced with the deeply inequitable situation of bearing the costs of removing waste they were not responsible for generating, contrary to the “polluter pays” principle (OECD, 1975).

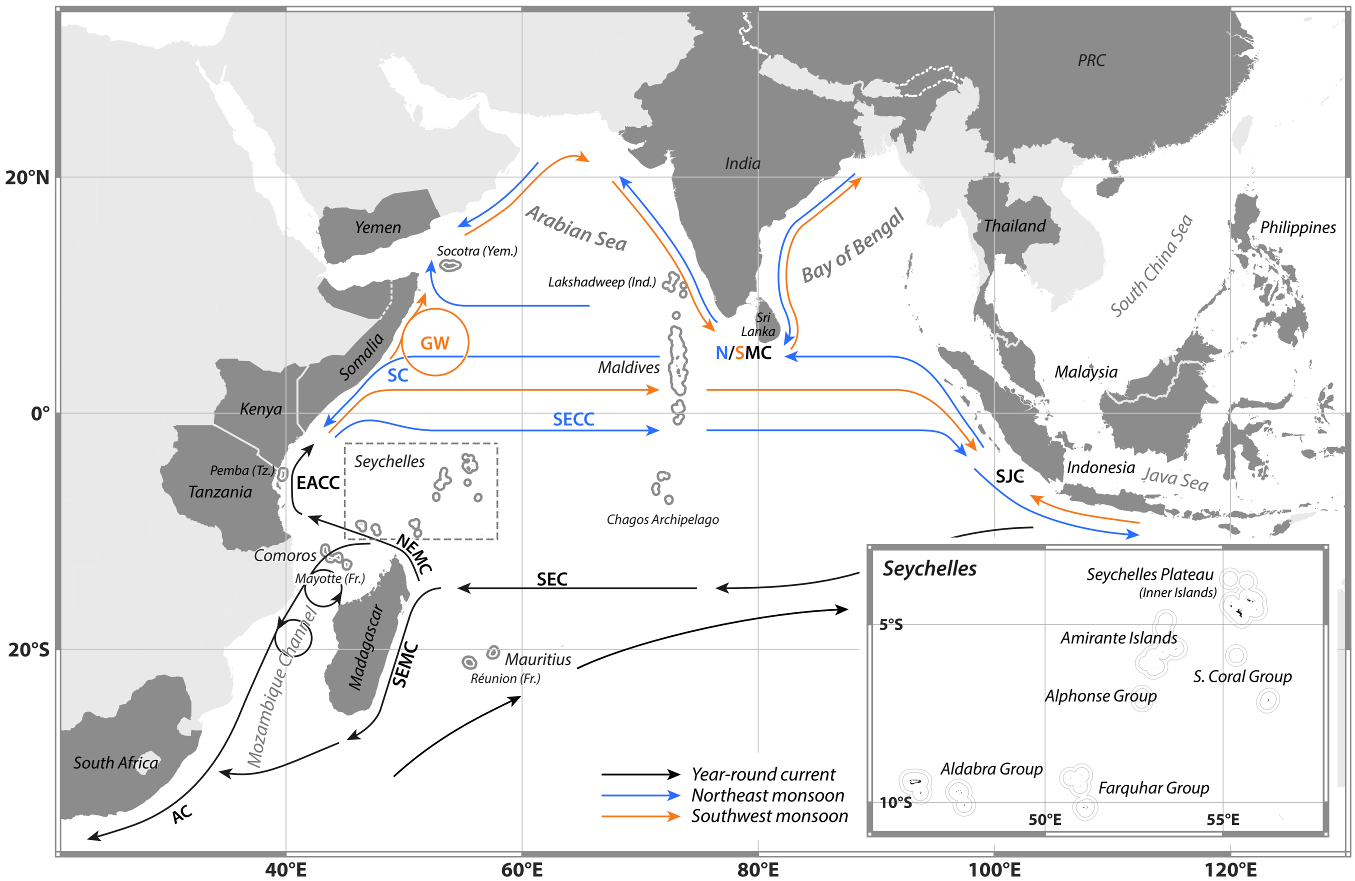

Figure 1: Map of the Indian Ocean, with key countries, island groups, and basins discussed in this study highlighted. Small islands are drawn with a halo for clarity. Arrows represent the major surface currents in the Indian Ocean, adapted from Schott et al. (2009). Black arrows represent currents that broadly occupy the same location year-round, whereas blue and orange arrows respectively represent currents during the northeast and southwest monsoon. *Inset:* The major island groups within Seychelles.

There are many small island developing states in the western Indian Ocean (Figure 1) and, whilst marine plastic pollution is under-studied in this region in comparison to, for instance, the North Atlantic and western Pacific, debris accumulation has been documented in many of these remote island groups. Seychelles is one such small island developing state, spread across over 100 islands north of Madagascar, from the isolated Aldabra Group in the southwest, to the Inner Islands on the Seychelles Plateau in the northeast. Marine debris monitoring programmes have found large quantities of marine debris accumulating across the latitudinal and longitudinal range spanned by Seychelles, such as at Aldabra Atoll (Burt et al., 2020), Alphonse Island (Duhec et al., 2015), Cousine Island (Dunlop et al., 2020), and many others (Macmillan et al., 2022). Marine debris is primarily of terrestrial origin at some of these sites (e.g. Alphonse Island, Duhec et al. (2015)) whereas abandoned, lost, or otherwise discarded fishing gear (ALDFG) of marine origin dominates at others (e.g. Aldabra Atoll, Burt et al. (2020)).

Attribution of marine debris accumulating at these remote islands would be a positive step towards accountability and prevention, but this is challenging. Several studies have inferred the sources of beached debris based on intact labels on bottles (e.g. Duhec et al., 2015; Burt et al., 2020), but this method has historically been limited to small sample sizes, is biased against debris lacking intact labels due to degradation and/or biofouling, and cannot give representative provenance information for all types of marine debris, as transport pathways vary greatly with debris geometry and composition (Duhec et al., 2015; Maximenko et al., 2018).

Numerical models can also be used to predict the source of beaching debris by representing debris as Lagrangian particles or Eulerian tracers. These simulations can be run forward-in-time, i.e. assuming knowledge of some input distribution of marine debris and predicting where that debris is transported (e.g. Kaandorp et al., 2020; van der Mheen et al., 2020; Chassignet et al., 2021), or backward-in-time, i.e. simulating trajectories that lead to a site of interest and inferring debris sources based on where debris passed through in the past (e.g. Duhec et al., 2015; Stelfox et al., 2020). In the context of marine debris attribution for remote islands, backward-in-time simulations are more efficient as they must only compute the small subset of trajectories that end at the site of interest, reducing computational cost. However, there are significant limitations associated with the backward-in-time approach. For instance, it is not possible to implement parameterisations for subgrid-scale diffusivity. Even more significantly, since simulated backward trajectories comprise an unknown subset of all possible trajectories, there are fundamental limitations on the quantitative constraints that can be obtained on the sources of marine debris. Most studies using backward-in-time simulations are limited to qualitative predictions of debris sources based on assumptions of a fixed drift time (e.g. Duhec et al., 2015). van Duinen et al. (2022) used a Bayesian framework to quantify sources of debris for a beach in the Netherlands, but this approach still relies on assumptions on how long debris were adrift before beaching. For remote islands where potential sources of debris are many and distal, it is challenging to justify any *a priori* assumption for a drift time distribution. An innovative approach was used by Stelfox et al. (2020), who predicted the source fisheries for ghost gear accumulating in the Maldives based on backward-in-time simulations and constraints on drift time from biofouling. Unfortunately, these constraints are likely debris-type and site specific, and no such estimates exist in general for most remote islands.

In the absence of constraints on drift time, forward-in-time simulations are required to provide quantitative, physically justifiable estimates for sources of marine debris. To date, sources of debris have been quantified for the Seychelles as part of two regional (van der Mheen et al., 2020) and global (Chassignet et al., 2021) studies. However, neither study registered a significant number of particles arriving at Seychelles, and they were therefore unable to make robust conclusions about sources of marine debris for remote islands. Both were large-scale studies focusing on major marine debris transport pathways, but this nevertheless highlights an important data gap, as well as a particular technical challenge for assessing sources of marine debris for small and remote locations.

As a result, whilst there are indications from bottle labels, no quantitative estimates exist for the relative importance of sources of debris for Seychelles, along with other remote island groups in the western Indian Ocean. Good constraints exist on source regions for one specific type of fishing gear, drifting Fish Aggregating Devices (dFADs), accumulating on Seychelles' beaches (Macmillan et al., 2022; Imzilen et al., 2021), but this has not been generalised to all marine-based sources of debris. In this study, we use large-scale Lagrangian forward simulations, forced by ocean currents, waves, and winds, generalisable to arbitrary sinking and beaching rates, to answer the following questions:

- Which countries are the most likely terrestrial sources of debris accumulating at Seychelles (and other western Indian Ocean islands), and how sensitive are these estimates to debris properties such as sinking rate and windage?
- If debris is generated at sea (from fisheries, ships, etc.), from which regions is there most risk of debris beaching at Seychelles, and can we therefore predict high-risk fisheries

and shipping channels?

- What are the physical drivers of marine debris accumulation at Seychelles, and are variations in accumulation rates (seasonal and inter-annual) predictable, allowing for more targeted cleanup efforts?

2. Methods

2.1. Particle tracking

To simulate the transport of marine debris, we carry out Lagrangian particle tracking using OceanParcels (Lange and Sebille, 2017; Delandmeter and van Sebille, 2019). Particles are tracked for 10 years or until the end of 2019, with trajectories integrated using a fourth-order Runge-Kutta scheme and a time-step of 1 hour. Over large scales, buoyant marine debris is transported by surface currents, Stokes drift, and in the case of debris protruding above the sea surface, windage (van Sebille et al., 2020), and all three processes are important in describing its dispersal (e.g. Duhec et al., 2015; Maximenko et al., 2018). We assume the force experienced by particles from the wind is parallel and proportional to surface winds, but note that this is a simplification compared to the real forces experienced by buoyant debris (Domon et al., 2012). We advect particles of terrestrial origin with 5 forcing scenarios: just surface currents (C0), surface currents + Stokes drift (CS0), and surface currents + Stokes drift + 1-3% windage (CS1-3). Particles of marine origin are advected using the same sets of forcing, plus 4% and 5% windage (CS4-5). We used the 1/12° CMEMS Global Ocean Physics Analysis GLORYS12V1 (Lellouche et al., 2021) for daily surface currents, 1/5° Global Wave Reanalysis WAVERYS (Law-Chune, 2021) for three-hourly Stokes drift, and 1/4° three-hourly surface winds from ERA5 (Hersbach et al., 2020) (all 1993-2019).

All three forcing sets are provided by CMEMS, regridded to a regular grid. We applied a homogeneous lateral diffusivity of 10 m^2 s^{-1} to particles, based on a typical value of the horizontal Smagorinsky diffusivity in the equatorial Indian Ocean diagnosed from GLORYS12V1 ((Smagorinsky, 1963), Supplementary Figure 1) and in line with previous studies (Okubo, 1971; Kaandorp et al., 2020). Further technical details on the treatment of particle tracking near the coasts are described in Supplementary Text 1.

2.2. Particle sinking and beaching

Marine debris is lost from the ocean surface through processes including beaching and sinking. These processes are complex and driven by small-scale physical and biological processes (van Sebille et al., 2020) and must therefore be parameterised in large-scale numerical models. Many models parameterise sinking as decay in the mass of debris represented by a particle (e.g. Kaandorp et al., 2020; Chassignet et al., 2021). Beaching is often parameterised by explicitly removing particles based on criteria, such as particles entering a land cell due to Stokes drift, wind and/or numerical error (e.g. Zhang et al., 2020; Cardoso and Caldeira, 2021), particle stagnation (e.g. Seo and Park, 2020; Bosi et al., 2021), or as a stochastic process associated with some probability (e.g. van der Mheen et al., 2020; Onink et al., 2021).

An advantage with modelling beaching as a stochastic process is the ability to incorporate complex behaviour such as resuspension (Liubartseva et al., 2018; Onink et al., 2021) and, as understanding of the physics of beaching improves, stochastic parameterisations will become an increasingly valuable tool. However, as these parameterisations remove Lagrangian particles from circulation (even if only temporarily), this can significantly reduce the number of particles representing floating debris in the model. This is a problem when attempting to quantify the sources of debris for small and remote islands: these islands are very small 'targets' and beaching events may be missed due to an insufficient number of particles, as was the case for Seychelles in the studies of van der Mheen et al. (2020) and Chassignet et al. (2021).

Instead, we assume that there is (i) a constant rate of debris removal through sinking, μ_s, and (ii) a constant rate of debris removal through beaching, μ_b^* when a particle is within a 1/12° coastal grid cell, and implement sinking and beaching offline through post-processing of the trajectory data. We store these beaching events for 18 sites within Seychelles (Aldabra, Assomption, Cosmoledo, Astove, Providence, Farquhar, Alphonse, Poivre, St Joseph, Desroches, Platte, Coëtivy, Mahé, Fregate, Silhouette, Praslin, Denis, and Bird). For our terrestrial-sourced debris experiments (section 2.3.1), we include an additional 9 sites from the wider western Indian Ocean (Comoros, Mayotte [France], Lakshadweep [India], Maldives, Mauritius, Réunion [France], Pemba [Tanzania], Socotra [Yemen], and the Chagos Archipelago). For brevity, we focus on Seychelles in this paper, specifically islands on the Seychelles Plateau, and the Aldabra Group as representative of the Outer Islands. Analyses and figures for other island groups that could not be included in this paper can be produced using the scripts in Supplementary Dataset 1.

By efficiently choosing which data to store during particle tracking simulations (see Supplementary Text 2), it is possible to compress all data required to reconstruct almost all beaching events from the over 2×10^{11} particles used across all our simulations in <1TB, whilst allowing key parameters to be varied through postprocessing without having to rerun simulations.

2.3. Debris sources

We classify marine plastic debris into terrestrial sources (debris that entered the ocean from coastlines) and marine sources (debris that entered the ocean at sea). Due to the relatively poor constraints on the input distribution and magnitude of marine sources, we use different approaches to consider terrestrial and marine sources.

2.3.1. Terrestrial debris sources

Debris can enter the ocean through rivers (transported from inland), as well as through direct coastal input from coastal populations through stormwater, sewage, or poor waste disposal (Mihai et al., 2022). For riverine debris input, we use the modelled midpoint annual estimates from Meijer et al. (2021), gridding the emissions from each river mouth to the nearest coastal cell on the 1/12° GLORYS12V1 grid (section 2.1). For direct coastal input, we base our estimates on modelled annual mismanaged plastic waste generation estimates from Lebreton and Andrady (2019). We degraded the resolution of this product to the GLORYS12V1 resolution, and then calculated emissions to the ocean by assuming that a fraction $f_i = f_c \cdot \exp\left[-\left(\frac{d_i}{L}\right)^2\right]$ of the mismanaged waste produced in a grid cell i enters the nearest coastal cell, where f_c is the maximum likelihood of mismanaged waste entering the ocean, d_i is the distance of cell i from the coast, and L is a length scale over which direct coastal input to the ocean is significant. This parameterisation is based on the assumption that waste is less likely to enter the ocean the further from the coast it is generated. Many previous studies have used the alternative assumption, inherited from Jambeck et al. (2015), that a fixed fraction of mismanaged waste generated within 50km of the coast enters the ocean. Both of these parameterisations are somewhat arbitrary, but we believe that our assumptions are more appropriate.

We set $L = 15$km to reflect the length scale of a typical coastal city. The parameter f_c is the main control on the ratio r of marine debris generation from coastal versus riverine sources. In the absence of good constraints on this parameter, we take $f_c = 0.25$, corresponding to a total flux of debris from coastal and riverine sources of 3.1 Mt y^{-1} and 1.0 Mt y^{-1} respectively ($r = 3.1$, between $r = 1.9$ in Kaandorp et al. (2020) and $r = 4.9$ in Lebreton et al. (2018)). The parameter f_c can, however, be modified during postprocessing and, if it becomes better constrained in the future, it is straightforward to regenerate our results for another value of f_c, or even an entirely different debris input distribution, using the trajectories in Supplementary Dataset 1.

To minimise the cost of simulations, we only considered coastal cells for countries that could reasonably act as a source of marine debris for islands in the western Indian Ocean, identified from a preliminary backward particle tracking experiment (Supplementary Text 3, Supplementary Figure 2). Many coastal cells were associated with a very small flux of debris, so we removed the 7773 (of 20742) coastal cells with the smallest contributions, leaving 99.99% of riverine plastic, and 99.9% of coastal plastic. An overview of the terrestrial sources of marine debris used in our experiments is shown in Figure 2.

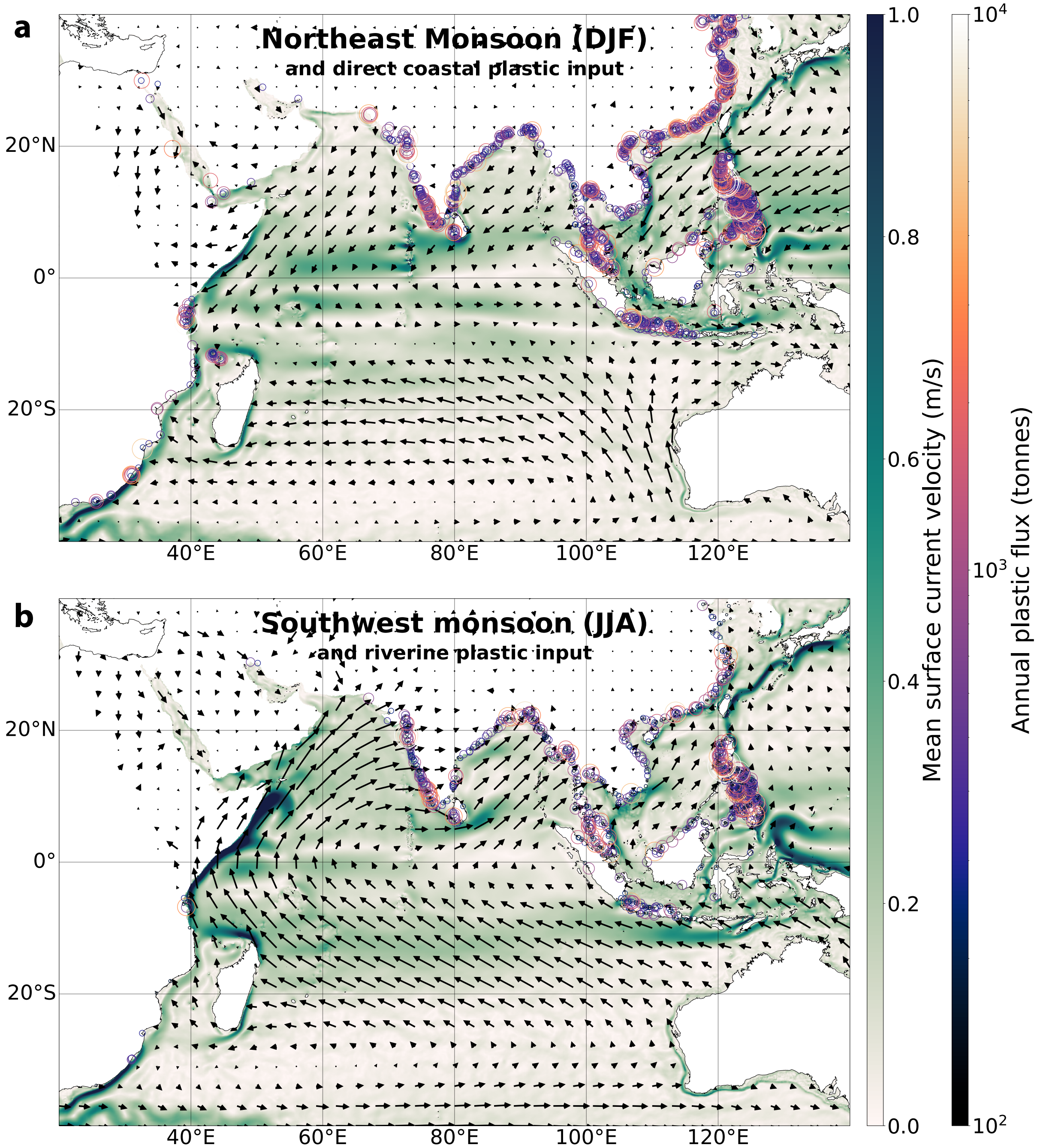

Figure 2: (a) Mean surface current speed (colours, Lellouche et al. (2021)) and surface winds (arrows, Hersbach et al. (2020)) for the northeast monsoon. Terrestrial sources of marine debris from direct coastal input, as used in our analyses, are overlaid, but note that this has no relation to the season. (b) Mean surface ocean current speed and surface winds for the southwest monsoon. Terrestrial sources of marine debris from riverine input are overlaid. This figure is zoomed to focus on the Indian Ocean region so does not include all sources of debris considered in the model; please see Supplementary Text 3 for a full list.

2.3.2. *Marine sources*

Global Fishing Watch uses tracking data from the automatic identification system (AIS), broadcast by large ships, to estimate fishing effort for tracked vessels (Kroodsma et al., 2018), which has been used as a proxy for ALDFG production in previous studies (e.g. Kaandorp et al., 2020). However, AIS coverage is poor in the Indian Ocean (Richardson, 2022). Instead, we use publicly available Indian Ocean Tuna Commission effort data for purse-seines and longlines (provided on 1° and 5° grids respectively), which is well-studied and has been used extensively as an indicator of fishing activity, particularly in the case of purse-seines (Kaplan et al., 2014; Imzilen et al., 2022). We consider longline fisheries from Japan, Taiwan, and Korea only, as data from these countries is the most reliable in terms of spatial distribution (Kaplan et al., 2014, Emmanuel Chassot (*personal communication*)). Since purse-seine and longline vessels lose gear at different rates (Kuczenski et al., 2022) with potentially different behaviour in the water, we do not aggregate effort from these two fisheries, and instead consider them separately.

From these fishing effort data, we can generate 'risk maps', representing where debris from a particular fishery beaching at a particular site is most likely to come from. This calculation requires a matrix $P_i(x, y, t_s, t_b)$ (for a particular debris class), giving the likelihood that debris beaches at site i in month t_b, given that it entered the ocean at (x, y) in month t_s; and a matrix $E_j(x, y, t)$, giving the fishing effort of fishery j at (x, y) in month t. The relative flux $f_{ij}(x, y)$ of fishery j debris from a point that *ever* beaches at site i is given by $f_{ij}(x, y) = \sum_{t_s=1}^{12} \left(E_j(x, y, t_s) \cdot \sum_{t_b=1}^{12} P_i(x, y, t_s, t_b)\right)$. We can normalise this relative flux by the total flux from all sources, to give the *risk* $R_{ij}(x, y)$ to site j from fishery i at location (x, y), $R_{ij}(x, y) = \frac{f_{ij}(x,y)}{\sum^{x,y} f_{ij}(x,y)}$. Along similar lines, we can also compute a monthly climatology $B_{ij}(t_b)$ for beaching rates from fishery j accumulating at site i, $B_{ij}(t_b) = \sum^{x,y} \left(\sum_{t_s=1}^{12} \left(E_j(x, y, t_s) \cdot P_i(x, y, t_s, t_b) \right) \right)$.

Debris may also be discarded or lost at sea from shipping traffic, which was suggested as a potentially significant source of debris for Alphonse Island, Seychelles by Duhec et al. (2015). This debris source is challenging to quantify, but we have used AIS-based estimates of shipping traffic intensity from Cerdeiro et al. (2020) as an indication of where major shipping lanes in the Indian Ocean are.

2.4. Seeding strategy

2.4.1. Terrestrial sources

For each coastal cell i on the GLORYS12V1 grid, we split the annual flux of debris of terrestrial origin F_i (as described in section 2.3.1) across 4 equally spaced releases per month, for a total of 48 identical releases per year. The debris associated with each release was further divided across n_i particles, such that the initial mass associated with a particular particle j released at cell i is $M_j^0 = F_i/48n_i$. We set $n_i = \lceil c_1 \cdot \log_{10} [F_i] - c_2 \rceil^2$, where $c_1 = 16$ and $c_2 = 18.4$ are arbitrary parameters chosen to distribute particles reasonably whilst keeping computation tractable. We released 13.7 million terrestrial particles per release event, for a total of 656 million per model year.

2.4.2. Marine sources

In each marine cell between 20°E-130°E and 40°S-30°N (excluding the Mediterranean) we generated 36 particles per release. As for terrestrial sources, we released particles at four equally spaced intervals per month, with 26.5 million particles per release event and a total of 1.27 billion particles per model year.

2.5. Debris Classes

In our model, the behaviour of marine debris in the ocean is set by the three parameters μ_s (sinking rate), μ_b^* (beaching rate), and the forcing scenario. No one set of parameters will describe all marine debris, and constraints on all three are poor. We explore the sensitivity of model results to this parameter-space in section 3.3.1, but to provide concrete examples, we have defined four representative debris classes:

- **Class A:** $1/\boldsymbol{\mu}_b = 30$d, $1/\boldsymbol{\mu}_s = 30$d, scenario **CS0**. Low volume mm-scale plastics with low (but positive) buoyancy and negligible exposure, e.g. **small plastic fragments, nurdles**.

- **Class B:** $1/\boldsymbol{\mu}_b = 30$d, $1/\boldsymbol{\mu}_s = 90$d, scenario **CS1**. Moderate volume cm-scale plastics with moderate positive buoyancy and minor exposure, e.g. **bottle caps, small domestic items**.

- **Class C:** $1/\boldsymbol{\mu}_b = 30$d, $1/\boldsymbol{\mu}_s = 360$d, scenario **CS3**. Moderate-large plastics with high positive buoyancy and moderate exposure, e.g. **beach sandals, bottles, foam sheets, buoyant nets.**

- **Class D:** (marine sources only) $1/\boldsymbol{\mu}_b = 30$d, $1/\boldsymbol{\mu}_s = 1800$d, scenario **CS5**. Large plastics with very high positive buoyancy and high exposure, e.g. **fishing debris with buoys attached, robust empty bottles.**

To derive these classifications, we used guidance on windage coefficients from Duhec et al. (2015) and Domon et al. (2012), sinking rates from Fazey and Ryan (2016), and beaching rates from our own analysis (Supplementary Text 4, Supplementary Figures 3-4) and Kaandorp et al. (2020). However, we stress that windage coefficients and sinking rates for different types of marine debris remain poorly constrained and the classes we have defined are suggestions only. All trajectories computed for this study (and scripts required to reproduce beaching rates) are provided in Supplementary Dataset 1, so practitioners can recompute predictions for parameters of interest.

2.6. Comparison with observations

Burt et al. (2020) estimated the total mass of debris that accumulated on Aldabra Atoll (Seychelles), as well as countries of origin for a small sample of PET bottles. Quantitative source analyses have also been carried out for Alphonse, Coëtivy, Astove and Platte (The Ocean Project Seychelles, 2019; Dunlop et al., 2020). Finally, Macmillan et al. (2022) analysed patterns of (satellite-tracked) drifting Fish Aggregating Device (dFAD) beaching events across Seychelles. We carried out a quantitative, side-by-side comparison of our analyses against the findings of these studies to identify limitations in both our approach, and these observational assessments of marine debris accumulation on remote western Indian Ocean islands.

3. Results and discussion

3.1. Sources of debris for remote islands in the western Indian Ocean

3.1.1. Debris of terrestrial origin

There is significant variation in the predicted source countries for debris beaching at the 27 sites investigated in this study (Figure 3). These figures can be interpreted as the predicted likelihood of a fragment of marine debris originating from the source country and beaching at the target island (group), given that it has properties reflecting Class A, B, or C debris as defined above.

For Class A debris (Figure 3(a)), East Africa (predominantly Tanzania) is expected to be the largest source of marine debris for most of the Outer Islands of Seychelles, although Comoros is the dominant source for Aldabra and Assomption. For the Inner Islands on the Seychelles Plateau, most Class A debris is expected to come from within Seychelles, with the remainder sourced from East Africa. For sites in the central-northern Indian Ocean (Maldives and Lakshadweep), India and/or Sri Lanka are expected to be the principal sources of debris. Only the Chagos Archipelago is predicted to source most of its Class A debris from Indonesia.

For Class B debris (Figure 3(b)), a combination of longer residence time at the ocean surface (3 months), westward Stokes drift, and easterly winds allows Indonesia to begin to dominate the marine debris budget for much of the western Indian Ocean. Our analyses predict that Indonesia is responsible for over 50% of all Class B debris for all Outer Islands of Seychelles (and remains the dominant source for the Chagos Archipelago). Seychelles and Tanzania are still expected to be significant sources of debris within the inner islands

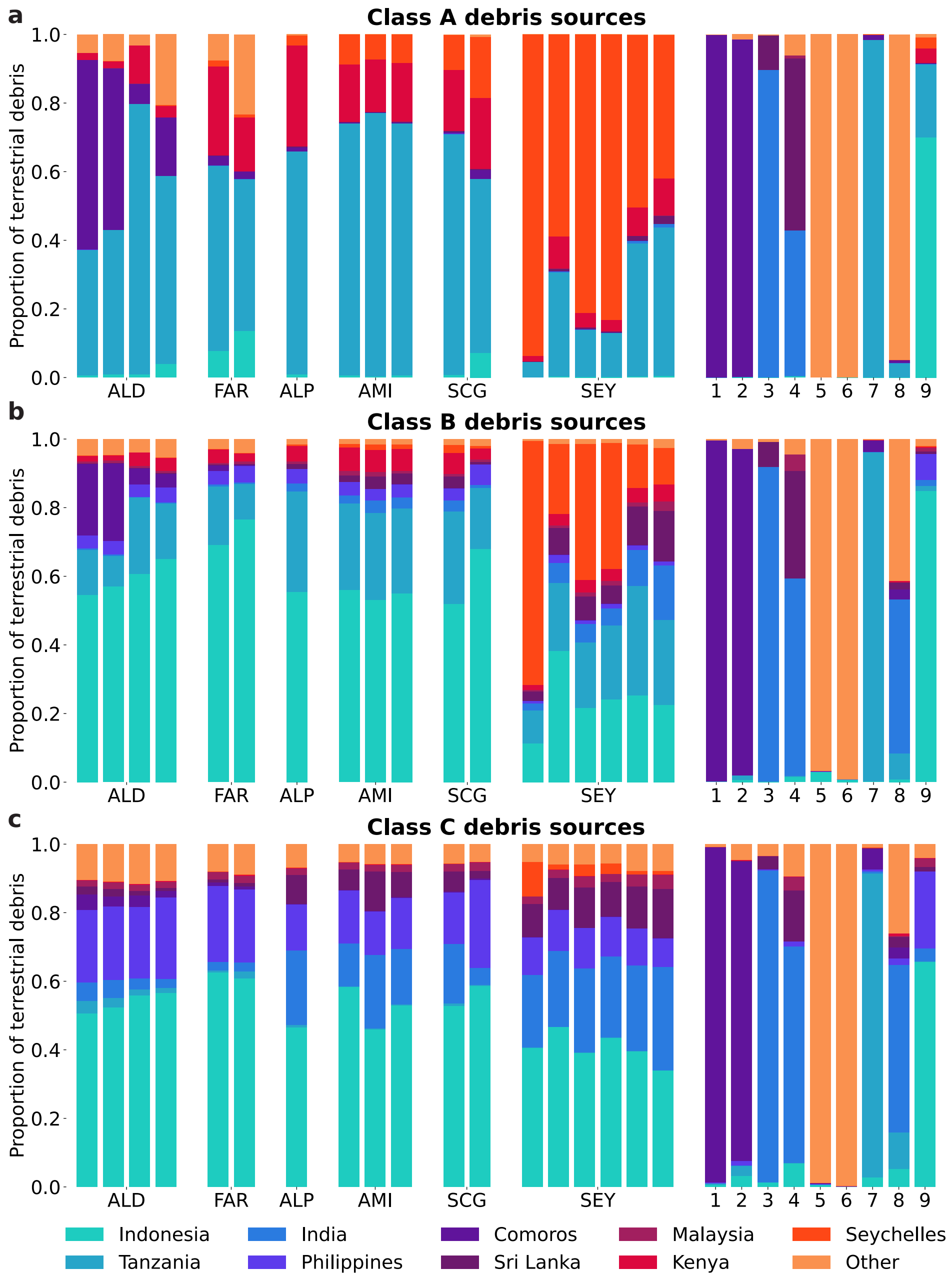

Figure 3: Sources of beaching (terrestrial) debris from all debris releases 1993-2014 for (a) Class A, (b) Class B, and (c) Class C debris. Sites from left to right: **Ald**abra Group (Aldabra, Assomption, Cosmoledo, Astove), **Far**quhar Group (Providence, Farquhar), **Alp**honse Group (Alphonse), **Ami**rante Islands (Poivre, St Joseph, Desroches), **S**outhern **C**oral **G**roup (Platte, Coëtivy), **Sey**chelles Plateau (Mahé, Fregate, Silhouette, Praslin, Denis, Bird); Comoros (**1**), Mayotte (**2**), Lakshadweep, India (**3**), Maldives (**4**), Mauritius (**5**), Réunion, France (**6**), Pemba, Tanzania (**7**), Socotra, Yemen (**8**), Chagos Archipelago (**9**). Nine source countries have been chosen; all other sources are grouped under 'other'. For sites with significant proportions of Class A debris from 'other' countries, the largest 'other' sources are as follows: Astove (Madagascar); Farquhar (Madagascar); Mauritius (Mauritius); Réunion (Réunion); Socotra (Yemen). For Class B debris: Mauritius (Mauritius); Réunion (Réunion); Socotra (Yemen). For Class C debris: Mauritius (South Africa and Mauritius); Réunion (Réunion and South Africa); Socotra (Yemen and Pakistan).

of Seychelles (particularly Mahé, the main population centre of Seychelles), but substantial proportions are also predicted to originate from Indonesia and, in the case of islands in the northernmost Seychelles Plateau (Denis and Bird islands), India and Sri Lanka. India and Sri Lanka are expected to still act as the main sources of debris for the relatively nearby island groups of Lakshadweep and Maldives, but the lower sinking rate and contributions from winds and waves during the northeast monsoon also results in these countries becoming significant sources of debris for Socotra, previously dominated by local sources from Yemen.

Finally, Class C debris (Figure 3(c)) beaching across Seychelles (and the Chagos Archipelago) is expected to originate almost entirely from the northern and eastern Indian Ocean. Indonesia is still expected to be the largest single source country, but a significant proportion is swept from Philippines and, in the case of more northerly islands, India and Sri Lanka. Seychelles and East Africa are not significant sources of Class C debris for any sites in Seychelles. Our analyses also suggest that Mauritius and Réunion, dominated by local sources for less-buoyant classes of debris, receive significant quantities of Class C debris from South Africa (57% and 36% respectively).

We can also extract the predicted drift time distribution for debris accumulating at our study sites (shown for Aldabra in Supplementary Figure 5). Unsurprisingly, the more buoyant debris classes have a broader range of drifting times, where drifting times are stratified by the oceanographic distance of source countries from Aldabra. For instance, for Class C debris accumulating at Aldabra, debris arriving from Comoros and Tanzania have generally only been at sea for 1-2 months, whereas debris arriving from Indonesia has been at sea for at least 6 months, with a small proportion exceeding 2 years. However, an important conclusion is that the distribution of drift times is complex and multimodal. Although Lagrangian back-tracking is considerably less computationally expensive than the approach used in this study, van Duinen et al. (2022) were required to make an *a priori* assumption for the drift time distribution of debris accumulating at their site of interest. These drift time distributions for Aldabra highlight that assuming a uniform age distribution of beaching debris is not an appropriate assumption for remote islands.

As further discussed in section 3.2, there is significant temporal variability in accumulation rates at many of these remote sites, particularly for Class A debris. However, recomputing Figure 3 for subsets of the full time-series suggests that our source attribution is robust for almost all sites (Supplementary Text 5).

3.1.2. Debris of marine origin

As with the terrestrial case, the probability of debris lost or discarded at sea eventually beaching at Seychelles strongly depends on the physical properties of the debris, and where it entered the ocean (Figure 4). Incoming Class A debris beaching at Aldabra (Figure 4(a)) is sourced from a relatively narrow latitudinal band, due to primarily zonal currents around Aldabra. The Class A risk region for the Aldabra Group is almost entirely eastward of the island group, as these islands are in the path of a powerful westward-flowing ocean current (the North Madagascar Current). In contrast, the Class A risk map for the Seychelles Plateau (Supplementary Figure 8) is centred on the plateau due to the monsoonal reversal of prevailing zonal currents around the island group (Schott et al., 2009).

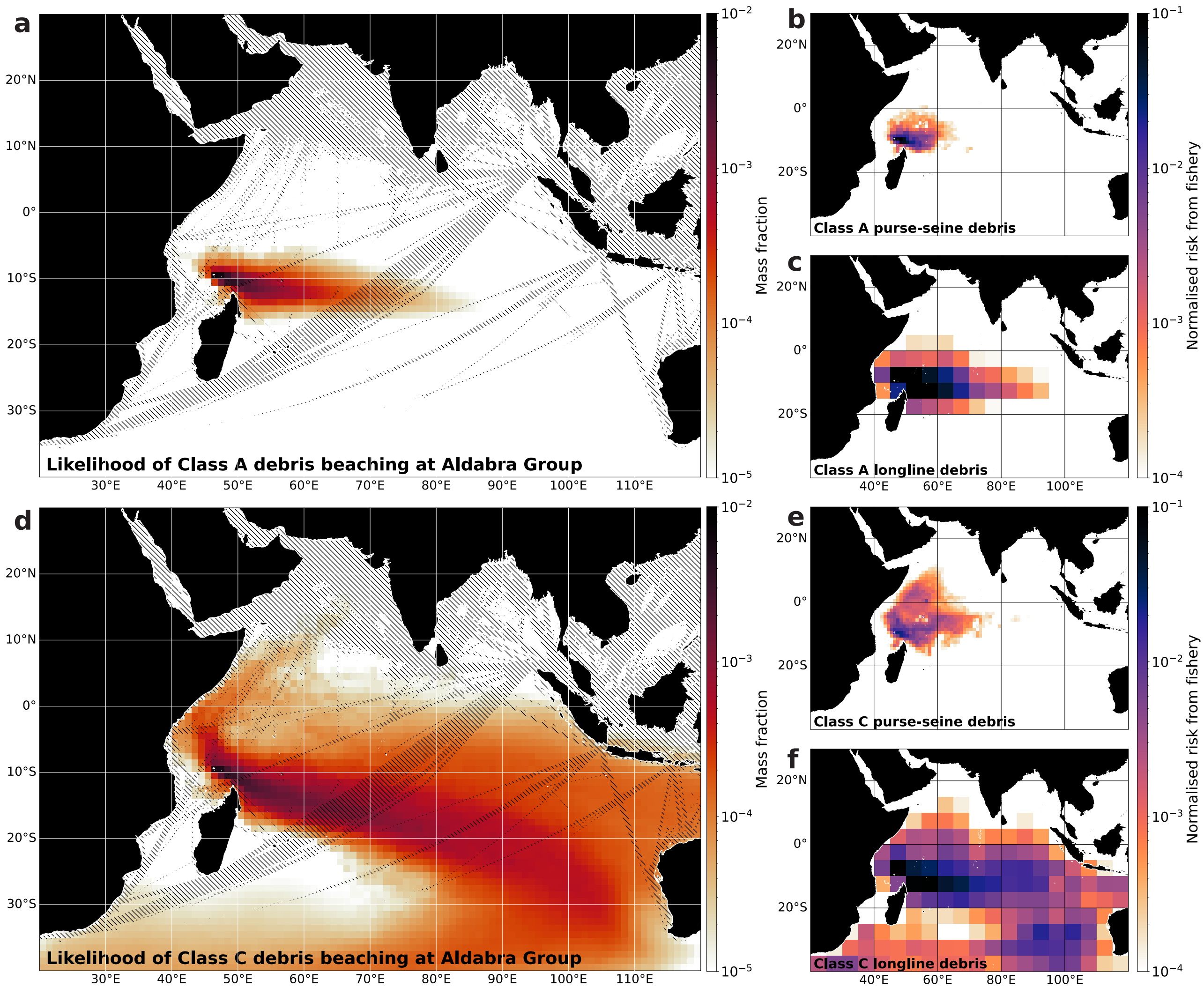

Figure 4: Risk map for Aldabra Group for (a) Class A debris and (d) Class C debris, showing the fraction of debris initialised per marine grid cell that beaches within the Aldabra Group. Hatching shows shipping corridors with the most intense traffic from Jan 2015 to Feb 2021 (Cerdeiro et al., 2020). Risk map for (b-c) Class A debris and (e-f) Class C debris from (b,e) purse-seines and (c,f) longlines ($R_{ij}(x, y)$ from section 2.3.2). Corresponding plots for the Seychelles Plateau can be found in Supplementary Figures 8-11. Note the logarithmic scales in all panels.

With a significantly longer residence time at the ocean surface, and greater propulsion due to windage, the risk maps for Class C debris (Figure 4(d)) cover a much greater area than for Class A debris. For both the Aldabra Group and Seychelles Plateau, debris from much of the tropical Indian Ocean has a non-negligible chance of beaching at one of these island groups. Although much debris in the Indonesian archipelagic seas and further afield is removed through beaching within the narrow straits of the Indonesian Throughflow, the sheer quantity of mismanaged waste generated in Indonesia and Philippines allows a significant quantity to leak into the Indian Ocean.

The right-hand side panels in Figure 4 show predictions of the relative risk to the Aldabra Group of ALDFG associated with purse-seine and longline fisheries. In the case of purse-seine debris, due to the concentration of fishing effort around the Seychelles, our analyses suggest that most debris originates from the western Indian Ocean. The seas around the Outer Islands of Seychelles are associated with the highest risk, but our analyses suggest that for Class C purse-seine debris, there is still a non-negligible risk from fishing activity to the north and east of the Seychelles Plateau (Figure 4(e)). In contrast to purse-seine fisheries, effort associated with longline fisheries is more broadly distributed around the Indian Ocean. As a result, the footprint of the potential source region is much larger than for purse-seines. In the case of longline ALDFG behaving as Class C debris, whilst the highest risk regions are still in the southwestern Indian Ocean (around Seychelles and eastern Madagascar), debris could reasonably be sourced from as far afield as the southeastern Indian Ocean, west of Australia (Figure 4(f)). This suggests that a significant proportion of ALDFG beaching at Seychelles could originate from outside the Seychelles EEZ, particularly in the case of longline debris.

Finally, Figure 4 also shows that there is significant overlap between major high seas shipping lanes (hatching in Figure 4), and high risk regions for Seychelles. Even in the case of short-lived Class A debris, the major shipping lanes linking the Bay of Bengal and South

China Sea to the Atlantic pass within the high risk zone for the Aldabra Group. For Class C debris, most of the major shipping lanes in the Indian Ocean pass through regions associated with a high risk of beaching for both the Inner and Outer Islands of Seychelles, including Atlantic-bound connections from the Middle East and Java Sea, as well as those originating from the Bay of Bengal and South China Sea.

3.2. Variability and drivers of beaching marine debris

Despite the monthly input of terrestrial debris remaining constant in our analyses, there is substantial temporal variability in beaching rate predicted for remote islands. Figure 5(a) shows the mass of Class A debris beaching at Aldabra (Aldabra Group) and Praslin (Seychelles Plateau) per month from 1995 (two years after the first debris release) to 2014 (the last release year for terrestrial debris). Although the average accumulation rate for Class A debris at Praslin is substantially higher than for Aldabra, the monthly accumulation rate at Aldabra varies over 6 orders of magnitude and its peak (in 1995) exceeds any month at Praslin. These patterns are a result of the different principal sources of Class A debris for Aldabra and Praslin (Figure 3(a)). In the case of Praslin, most Class A debris is sourced from within Seychelles, largely from Mahé (around 50km away). The transport pathway from source to sink for Class A debris beaching at Praslin is therefore short ($<$ 2 weeks), which allows debris from within Seychelles to consistently beach at Praslin before sinking, with less of an opportunity for seasonal variations in ocean currents or eddy variability to disrupt this pathway. In contrast, most Class A debris beaching at Aldabra originates in Comoros and Tanzania, both of which are hundreds of kilometres away and are connected to Aldabra through low probability connections (Figure 4(a)). As a result, Aldabra sees almost no Class

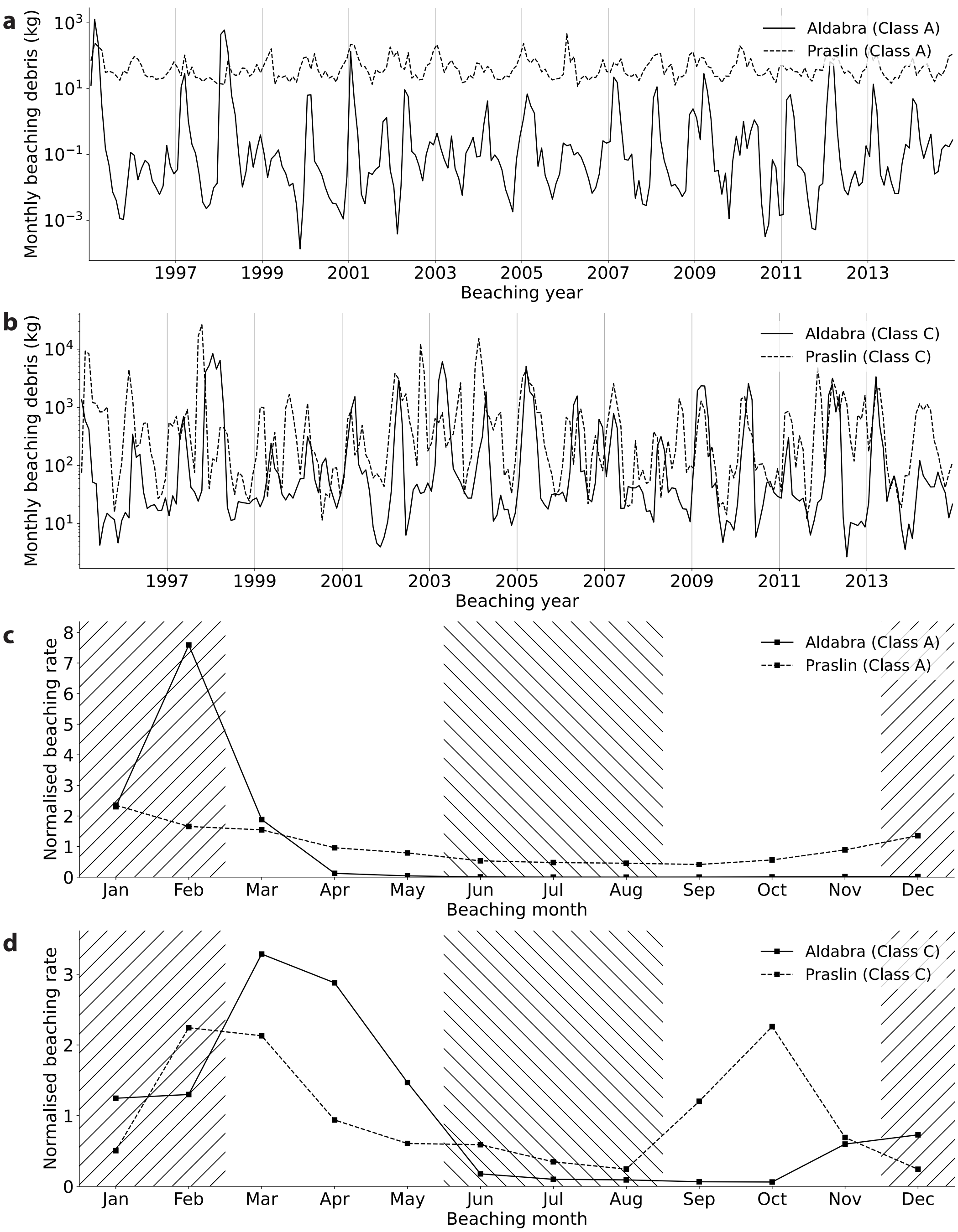

Figure 5: (a)-(b) Monthly beaching rate from 1995-2014 at Aldabra (Aldabra Group) and Praslin (Seychelles Plateau) assuming all terrestrial debris is (a) Class A and (b) Class C. (c)-(d) Monthly beaching rate averaged across 1995-2014 at Aldabra and Praslin (normalised by the annual mean) for (c) Class A and (d) Class C debris. The hatching indicates the approximate timing of the northeast monsoon (∼ December to February) and southwest monsoon (∼ June to August).

A debris beaching in most months, but if an eddy happens to direct a filament of Class A debris towards Aldabra, a large amount of debris may beach in a short period of time. This prediction is similar to patterns of 'pulsed recruitment' predicted for the long-distance larval dispersal of some marine organisms (e.g. Siegel et al., 2008).

In contrast, *both* Praslin and Aldabra see a similar level of variability in beaching rates for Class C debris (Figure 5(b)). Most Class C debris beaching at both islands originates from distal sources in southeast Asia and, in the case of Praslin, south Asia. Class C debris arrives at both islands through long-distance transport pathways, and there is therefore ample opportunity for these transport pathways to be controlled by stochastic, eddy-induced variability. The variability in accumulation rate at Aldabra is lower for Class C debris than for Class A, possibly because the wider geographic distribution of sources and greater time available for mixing 'smooths out' the distribution of marine debris in the ocean. Nevertheless, monthly beaching rates for both islands are predicted to vary across three orders of magnitude, with most debris arriving during short periods of high accumulation rate.

3.2.1. Seasonal variability

Given this enormous variability in beaching rate, it is useful to understand whether beaching rate varies entirely stochastically, or whether there is some predictability (which could help with the organising of beach clean-ups and other marine debris management activities). In particular, prevailing winds and many currents in the Indian Ocean change direction following the monsoons[1]. These monsoons have previously been suggested to control the partitioning of debris between the southern and northern Indian Ocean (van der Mheen et al., 2020). Figures 5(c)-(d) show the monthly accumulation rate for Class A and C debris

[1]In this study, we refer to the monsoons around December to February, and June to August, as the northeast and southwest monsoons, respectively, in line with Schott et al. (2009).

arriving at Aldabra and Praslin, averaged over the interval 1995-2014. For Class A debris (Figure 5(c)), almost all debris beaches at Aldabra between January and March, i.e. the end of the northeast monsoon. The sharpness of this peak is partially due to extreme events in 1995 and 1998 (Figure 5(a)), but this seasonal cycle remains robust even without these years. Comoros is the largest source of Class A debris for Aldabra but ordinarily, debris from Comoros is swept into the Mozambique Channel and away from Aldabra. Rapid debris transport from Comoros to Aldabra relies on a relatively uncommon pathway in which debris is entrained into eddies in the northern Mozambique Channel and transported towards Madagascar, before entering the North Madagascar Current upstream of Aldabra, and subsequently beaching. This pathway is improbable during the southwest monsoon as a strong North Madagascar Current Backeberg and Reason (2010) results in debris rapidly beaching along the east African coast. As a result, transport from Comoros to Aldabra is generally only feasible during the northeast monsoon and subsequent intermonsoon. There is some seasonal variability at Praslin, with higher Class A beaching rates during the northeast monsoon, but considerably less than Aldabra. During the northeast monsoon, the South Equatorial Countercurrent shifts towards the south near the Seychelles Plateau (Schott et al., 2009), facilitating the eastward transport of debris from the highly populated island of Mahé towards Praslin. Conversely, the South Equatorial Countercurrent shifts to the north during the southwest monsoon, and debris is more likely to be transported westward from Mahé due to the northwestward Stokes drift over the Seychelles Plateau at this time. Indeed, the seasonal pattern for Class A debris beaching at Silhouette Island, west of Mahé, is in exact antiphase to the pattern at Praslin (see Supplementary Table 1).

In the case of Class C debris, both Aldabra and Praslin see a peak in beaching rate during the late northeast monsoon and subsequent intermonsoon (Figure 5(d)). In the case of Aldabra, this peak is due to debris from Indonesia, whereas the peak at Praslin is due to debris arriving from India and Sri Lanka. Instead, Praslin has a second Class C beaching peak following the southwest monsoon, which is driven by debris from Indonesia. However, this peak is deceptive. Contrary to Aldabra, which has a clearly defined peak attributable to Indonesia at approximately the same time in almost all model years, the time-mean peak attributable to Indonesia at Praslin in Figure 5(d) is actually driven by a small number of outlier events, most significantly in 1997. Although the time-integral source attribution data presented in Figure 3 are generally robust with respect to simulation timespan, it is clear through inspection that interpreting temporal variability in beaching rate is not as straightforward.

Alternatively, we can observe that, in most years, log-transformed beaching rates are dominated by a single clear sinusoidal peak at most sites we considered (e.g. Figure 5(a)). By analysing beaching rates in the frequency domain and extracting the phase of the component with a period of 1 year, we can estimate during which season beaching rates *consistently* peak. This is summarised for Class C debris in Table 1 (corresponding tables for Class A and Class B debris are given in the Supplementary Tables 1-2). To verify whether the assumption of a single clear beaching rate peak per year is valid, we computed the correlation between the actual (log) beaching rate, and the idealised beaching rate using only the annual component of the Fourier spectrum. This correlation was significant ($p < 0.01$, taking into account autocorrelation within both the modelled and seasonal time-series (Bretherton et al., 1999)) for almost all islands considered.

Table 1 suggests that the seasonality of beaching rates across Seychelles is actually in phase for Class C debris of terrestrial origin, with a significant peak predicted in March or April for almost all Seychellois islands (i.e. the end of the northeast monsoon and the subsequent intermonsoon). This peak shifts slightly earlier in the year for less buoyant classes, but remains during the northeast monsoon for Class A and Class B debris beaching at most islands in Seychelles. The strength of this seasonality (quantified by the ratio of the beaching rate during the highest and lowest three months), however, is considerably larger for the Outer Islands of Seychelles, particularly for the Aldabra, Farquhar and Alphonse Groups.

We can gain further insight into the physical drivers of this seasonality by repeating the same spectral analysis for all source grid cells in the marine-release experiments. Plotted in Figure 6(a) is the correlation between the beaching time at the Aldabra Group of debris released across the Indian Ocean, and the seasonal cycle identified for that cell from the Fourier Spectrum. Although our analyses suggest that Indonesia is the dominant source of Class C debris for Aldabra, Figure 6(a) shows that debris beaching at the Aldabra Group is significantly correlated ($p < 0.01$) with the seasonal cycle for most source regions across the Indian Ocean, as well as the Indonesian archipelagic and Chinese marginal seas. The phase of this seasonal cycle is given in Figure 6(b), revealing that this entire region is perfectly in phase. This may be surprising, as the drift time to the Aldabra Group varies considerably across the Indian Ocean. If the seasonality of Class C debris beaching at the Aldabra Group depended on remote forcing (i.e. currents, winds and waves at the debris source region, or

Beaching site	Seasonal cycle peak	Seasonality strength
Aldabra	March	35.1
Assomption	March	36.7
Cosmoledo	March	35.1
Astove	March	35.2
Providence	March	48.3
Farquhar	March	47.4
Alphonse	March	39.0
Poivre	April	13.6
St Joseph	March	10.9
Desroches	April	8.7
Platte	March	6.3
Coëtivy	*March*	*20.1*
Mahé	March	5.2
Fregate	April	6.3
Silhouette	April	10.5
Praslin	March	8.0
Denis	April	5.7
Bird	April	6.9
Comoros	December	1.9
Mayotte	January	18.7
Lakshadweep	February	92.4
Maldives	February	10.7
Mauritius	*August*	*1.9*
Réunion	*November*	*1.3*
Pemba	January	4.4
Socotra	March	12.7
Chagos Archipelago	September	7.9

Table 1: Class C debris beaching rate seasonal peak, and strength of the seasonal cycle (1995-2014), based on the phase of the component of the Fourier spectrum with period 1 year. The strength of the seasonal cycle is the ratio of the mean beaching rate during the three months with the highest beaching rate, and the three months with the lowest beaching rate. All time series correlated significantly with idealised cycle ($p < 0.01$) aside from sites in *italics*.

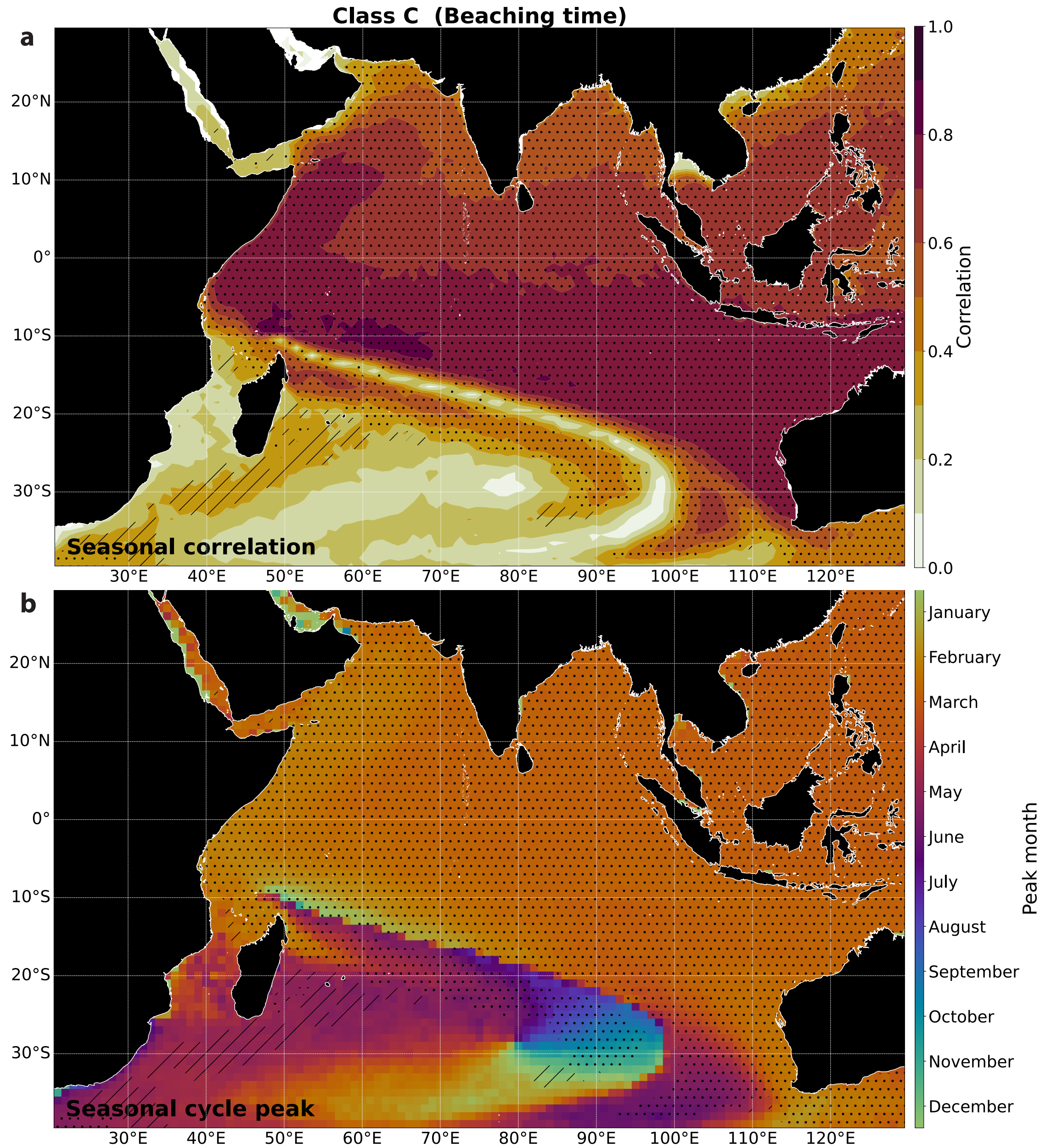

Figure 6: (a) Correlation between (log-transformed) time-series of debris beaching at the Aldabra Group from each cell, and the idealised seasonal cycle extracted from the Fourier spectrum. Shading indicates that the time-series in a cell correlates with the seasonal cycle significantly, $p < 0.01$ (dotted) and $p < 0.05$ (hatched), taking into account autocorrelation within both the modelled and seasonal time-series (Bretherton et al., 1999). (b) Phase of the seasonal cycle extracted from the Fourier spectrum, in terms of the seasonal cycle peak.

along its transport path), we would expect considerable spatial heterogeneity in Figure 6(b).

Instead, this figure demonstrates that the seasonality of Class C debris beaching at the

Aldabra Group is dominated by *local* forcing, specifically the monsoonal variation in the winds. During the northeast monsoon, winds around Aldabra are relatively weak (Figure 2(a)) and westward zonal surface currents are proportionately more important. As a result, debris arriving at Aldabra during the northeast monsoon is sourced, on sub-seasonal timescales, east of Aldabra, from the southern tropical Indian Ocean. Conversely, during the southwest monsoon, strong southeasterly winds blow over the Aldabra Group (Figure 2(b)) and the source region for Aldabra (on sub-seasonal timescales) shifts to the *south*east of Aldabra, in the southern *sub*tropical Indian Ocean. Crucially, since winds over the southern Indian Ocean never have a strong northerly component (Figure 2), there is *no efficient pathway* for Class C marine debris to reach the subtropical southern Indian Ocean from Indonesia (or other south(east) Asian sources), and therefore no route to Aldabra. As a result, it is improbable for Class C debris from the eastern or northern Indian Ocean to reach Aldabra during the southwest monsoon. This wind-driven mixing barrier can be clearly seen in Figure 6(b) as the sharp phase discontinuity extending southeastwards from the Aldabra Group.

In this way, the monsoonal winds over the Aldabra Group act as a debris 'switch', alternating the principal debris source between the southwestern Indian Ocean (with minimal debris sources), and the remainder of the basin. The dominance of winds over the seasonality of beaching at the Aldabra Group remains valid for Class B debris, but not for Class A debris (0% windage), where the seasonality instead appears to be dominated by the strength and position of the North Madagascar and South Equatorial Currents. The phase of the seasonal cycle with respect to the Seychelles Plateau (Supplementary Figure 17) is similar to the Aldabra Group, but due to the more northerly position of the Inner Islands, winds associated with the southwest monsoon do not have as extreme a blocking effect as with the Aldabra Group. Additionally, as hinted at by the greater spatial heterogeneity in Supplementary Figure 17, remote forcing may play a greater role for debris beaching at the Inner Islands. For instance, there is a fairly direct transport pathway from India and Sri Lanka to the Seychelles Plateau during the northeast monsoon due to the northeasterly winds and westward-flowing Northeast Monsoon Current south of India, whereas these winds and currents reverse during the southwest monsoon.

At some remote islands, such as Aldabra, most beaching debris is actually related to fishing activities rather than terrestrial input (Burt et al., 2020). As a result, the seasonal patterns identified for Aldabra may not necessarily be the same for fishing-related debris due to the very different input distribution to debris from the coasts. However, by computing monthly beaching rates for ALDFG ($B_{ij}(t_b)$ from section 2.3.2), we find that, although peaks are not perfectly aligned with predictions for debris of terrestrial origin, purse-seine and longline associated debris beaching at the Aldabra Group will still likely peak during the northeast monsoon or subsequent intermonsoon, and fall to a minimum during the southwest monsoon (Figure 7(a)-(b)). As a result, although there may not be a clearly defined peak of debris accumulation at Aldabra in March as suggested by Table 1, we would still expect debris accumulation to be significantly enhanced during the northeast monsoon and subsequent intermonsoon, as compared to the southwest monsoon. For fishery-related debris accumulating at sites across the Seychelles Plateau, our analyses suggest that the seasonal cycle would be similar, but slightly broader and shifted later in the year. This may be due to the more central position of the Seychelles Plateau with respect to intensive fisheries in

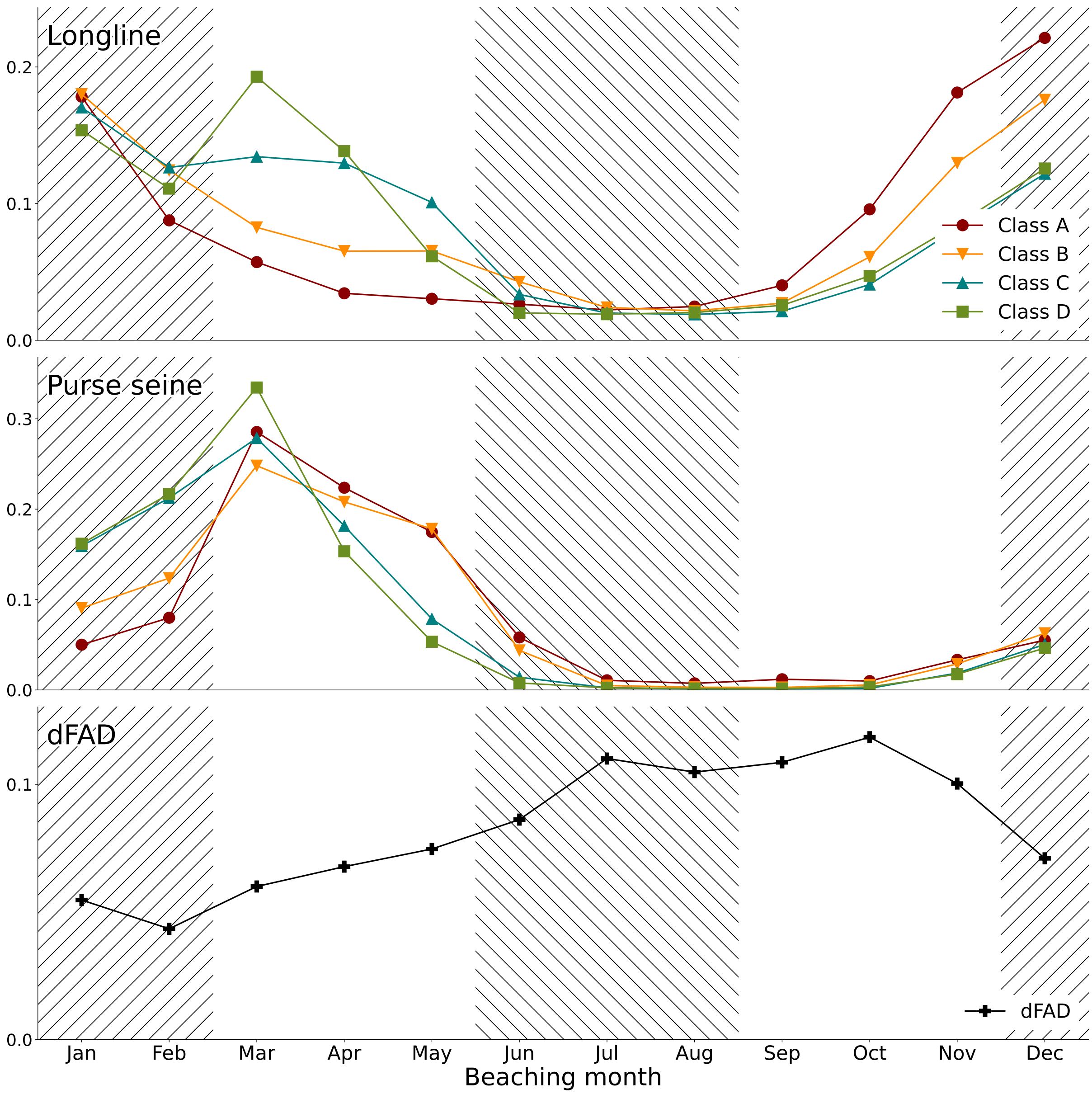

Figure 7: (a)-(b) Monthly beaching rate from 1995-2012 at the Aldabra Group for debris related to (a) longlines and (b) purse-seines, for Class A-D debris. (c) Predicted monthly beaching rate of dFADs, assuming they are not affected by winds or Stokes drift, i.e. follow physical scenario **C0** (Imzilen, 2021). Supplementary Figure 19 is the analogous plot for the Seychelles Plateau.

the western Indian Ocean, as well as the seasonality of fishing activities in the region, which is incorporated into these analyses.

3.2.2. Interannual variability

Although our analyses suggest that temporal variability in beaching rates at remote islands in the western Indian Ocean is dominated by seasonal variability from the monsoons, there is still considerable interannual variability. This is most extreme in the case of the short-lived Class A debris, where for some islands the majority of beached debris arrived during a small number of debris pulses. However, even in the case of the more predictable and long-lived Class C debris, inspection of Figure 5(b) demonstrates that substantial year-to-year variability remains. Northerly wind anomalies across the southern Indian Ocean are associated with IOD and ENSO events (Yu et al., 2005) and, as described in Section 3.2.1, the meridional component of winds over the southern Indian Ocean associated with the monsoons appear to be driving the seasonal cycle in beaching rates across Seychelles. We may therefore expect IOD and ENSO phases to amplify the seasonal cycle simulated for Seychelles, amplifying northeast monsoon beaching rates for debris from southeast Asia during positive phases, and further suppressing southwest monsoon beaching rates during negative phases.

To test this, we passed time-series of marine debris beaching rates through a low-pass filter with a cutoff frequency of 1.25 years, to remove intra-annual variability from the signal. We then carried out a lagged correlation of the filtered time-series against the Dipole Mode Index (DMI), an IOD index based on SST gradients across the equatorial Indian Ocean, and NINO3.4, an ENSO index based on mid-Pacific SST. Figure 8(a) shows an analogue of Figure 6(a) based on correlations of Class C debris beaching rates at the Aldabra Group with DMI. Although correlations are unsurprisingly lower than for the seasonal cycle, interannual

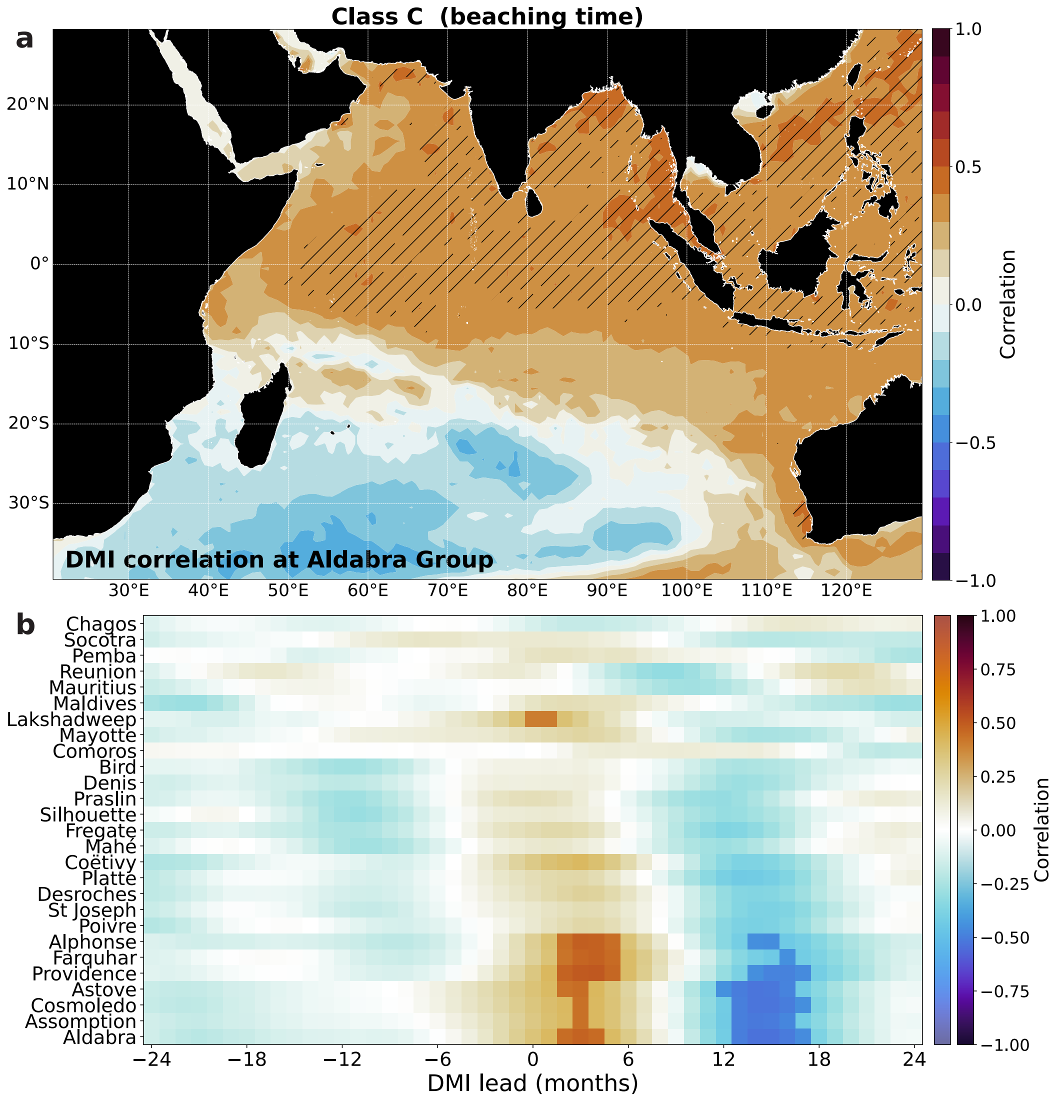

Figure 8: (a) Correlation between (log-transformed) time-series of debris beaching at the Aldabra Group from each cell, and the IOD Dipole Mode Index (DMI). Shading indicates that the time-series in a cell correlates with DMI significantly, $p < 0.01$ (dotted) and $p < 0.05$ (hatched), taking into account autocorrelation within both the modelled and DMI time-series (Bretherton et al., 1999). (b) Correlation between the (log-transformed) time-series of debris beaching at each site investigated in this study, and DMI, as a function of DMI lead time (months). Correlations significant to $p < 0.01$ are shown in bolder colours (the second colour bar).

variability in Class C beaching rates at Aldabra are correlated with DMI for source sites across much of the north and northeastern Indian Ocean. Additionally, the spatial pattern of these correlations strongly resembles the pattern in Figure 6(a) from the seasonal cycle, supporting the hypothesis that the IOD may amplify the seasonal cycle through modulation of meridional winds in the southern Indian Ocean. Figure 8(b) shows correlations between the total Class C beaching rate at all sites considered in this study, and DMI, as a function of DMI lead time. DMI correlates significantly with beaching rates at islands in the Aldabra, Farquhar, and Alphonse groups, which is expected as these are the same island groups that saw the most dramatic modulation by the seasonal cycle. DMI also correlates most strongly with beaching rates with a lead time of a few months, which supports the hypothesis that the IOD modulates the seasonal cycle as the monsoonal winds also lead peak Class C beaching rates (the seasonal cycle peaks in Table 1 within Seychelles generally occur just after the northeast monsoon, during the subsequent intermonsoon).

Correlation with the NINO3.4 index actually returns higher correlation coefficients compared to DMI, which is consistent with the partial correlations with the surface wind field given in Yu et al. (2005), as ENSO appears to be associated with stronger meridional wind anomalies closer to Aldabra. However, due to the longer autocorrelation timescale within the NINO3.4 time-series, the correlation of the NINO3.4 index with beaching rates at our study sites was not significant ($p > 0.01$).

3.3. Comparison with observations

3.3.1. Marine debris accumulation at Aldabra

The two parameters in our analyses describing the sinking rate and beaching rate, μ_s and μ_b^*, are highly uncertain, particularly μ_s. Fazey and Ryan (2016) estimated sinking timescales for polyethylene (LDPE and HDPE) fragments ranging from 0.5-5cm in size and, whilst the statistical model used in their study is not identical to the statistical model used for our sinking parameterisation, they estimated sinking timescales on the order of 17-66 days. Kaandorp et al. (2020) predicted a slightly higher sinking timescale of $1/\mu_s = 81$ days based on an inverse model incorporating observations of floating debris in the Mediterranean Sea. Koelmans et al. (2017) predicted an effective removal timescale of marine debris from the ocean surface (through fragmentation into microplastics) on the order of months, based on mass-balance arguments and observations of floating debris. However, Lebreton et al. (2019) argued that observations of the age distribution of debris in the North Pacific subtropical gyre are inconsistent with rapid sinking rates, instead suggesting that observations are more consistent with low sinking rates and rapid scavenging of debris at coastlines through beaching.

There are very few observational estimates for marine debris beaching rates. Dunlop et al. (2020) carried out repeat beach surveys at Cousine Island, Seychelles, from 2003-2019, and estimated accumulation rates. However, they calculated accumulation rate in terms of number of items rather than mass, so these results cannot be directly compared to our model output. However, Burt et al. (2020) carried out a five-week clean-up on Aldabra, Seychelles, and estimated that 513.4 tonnes of debris had accumulated on the island, of which 87.3 tonnes was terrestrial in origin. Annual emissions of marine debris into the ocean have increased over time, but our numerical model assumes constant annual debris emissions at 2015 levels. We estimate that the 87.3 tonnes of terrestrial debris that has accumulated at Aldabra corresponds to an annual beaching rate of around 2.9-5.3 tonnes per year, assuming no losses (see Supplementary Text 6).

Calculating the average annual beaching rate at Aldabra across μ_b^*-μ_s parameter space (from 1999-2014 to allow a longer spin-up for lower values of μ_s) reveals (1) that the beaching rate at Aldabra is insensitive to beaching rate in the interval $1/\mu_b^* \in [5, 60]$, and (2) that the inferred average bulk beaching flux at Aldabra is most consistent with 100d $< 1/\mu_s <$ 400d, depending on the windage coefficient (Supplementary Figures 20-22). This is not to suggest that all marine debris has a sinking rate in this range (μ_s is a variable which will likely depend on debris composition, geometry, and biofouling rates), but it does indicate that most debris, by mass, is likely to have a sinking rate on the order of months to a year. This is consistent with the findings of Fazey and Ryan (2016), Kaandorp et al. (2020), and Koelmans et al. (2017). As a result, Class A debris is probably not going to represent a significant fraction of debris beaching at Aldabra by mass. Additionally, it is also unlikely that most debris beaching at Aldabra has a sinking timescale of multiple years, since we would expect a significantly greater mass of terrestrial debris to have accumulated on Aldabra if this were the case.

3.3.2. Temporal variability of marine debris beaching across Seychelles

Drifting Fish Aggregating Devices (dFADs) are buoyant drifters used primarily by purse-seine fisheries to aggregate tuna. The majority of these dFADs are tracked remotely using satellite-transmitting GPS-equipped buoys and as a result, dFADs are one of the only types of marine debris that can be tracked directly from source to sink Imzilen et al. (2021). Macmillan et al. (2022) identified over 3000 dFAD beaching events across Seychelles, and analysed beaching rates and seasonality. This provides a useful test-case for our trajectory analysis, but the physics of dFAD transport do not correspond well to any of our marine debris classes A-C; the long drogue attached to dFADs reduces the effects of windage and Stokes drift, and a previous study found that the incorporation of windage reduces the skill score of dFAD trajectory prediction (Imzilen, 2021). As a result, we define 'dFADs' as a new Class of marine debris with $\mu_s = 1800$d (dFADs are large, buoyant, and non-biodegradable), $\mu_s = 30$d, and physical scenario **C0** (surface currents only. Imzilen (2021)). We compute the predicted seasonal distribution of dFAD beachings based on the methodology described in section 3.2.1, taking into account the seasonality of dFAD deployments. Our simulations reproduce a relatively muted seasonal cycle of dFAD deployments at Aldabra (Figure 7(b)) and a pronounced peak in dFAD beaching rates within the Seychelles Plateau during the intermonsoon following the northeast monsoon, both of which correspond well to observations (Isla MacMillan, *personal communication*).

3.3.3. Sources of debris at remote islands in the western Indian Ocean

Aldabra (Seychelles)

In addition to quantifying the total mass of debris on Aldabra, Burt et al. (2020) also identified the origin of 45 PET bottles with intact labels. In Table 2, we compare the predicted distribution of countries of origin for Class C debris beaching at Aldabra, to the distribution of countries of manufacture for intact PET bottles found at Aldabra.

For several countries of origin, there is agreement between the two datasets. Of the 5 largest sources of debris predicted by the model, bottles were found on Aldabra from 3 (Indonesia, India, and South Africa). Indonesia was the largest source of (Class C) debris in our model,

Origin	This study (%)	Burt et al. (2020) (%)
Indonesia	50.6	13.3
Philippines	21.2	-
India	5.3	6.7
South Africa	5.0	2.2
Comoros	4.4	-
Tanzania	3.7	-
Sri Lanka	2.4	-
Timor-Leste	1.7	-
Malaysia	1.6	6.7
Thailand	0.5	8.9
China	<0.1	46.7
Singapore	<0.1	4.4

Table 2: Distribution of countries of origin or manufacture from this study (based on Class C debris) and the sample of 45 PET bottles with intact labels from Burt et al. (2020). Only countries associated with at least 1% of accumulated debris (this study) or at least 1 bottle (Burt et al., 2020) are included.

and was the second largest country of manufacture in the sample from Aldabra. However, there are also some significant differences. This in itself is not unexpected. For instance, the sample size (45) of PET bottles in Burt et al. (2020) is small, and the sample is likely biased against bottles with longer drift times, as only bottles with intact labels could have their country of manufacture identified. Additionally, the country of manufacture of a bottle is not necessarily the same as the country where a bottle entered the ocean. However, the particular countries associated with model-observation disagreement provide interesting insights into the sources of debris for Aldabra.

The most obvious discrepancy between the two datasets is China. In our analysis, China was responsible for a negligible proportion of Class C debris accumulating at Aldabra (<0.1%), but was responsible for the manufacture of almost half of all bottles actually found on Aldabra. Although our Class C debris may be an imperfect representation of the physics driving PET bottle transport, no realistic combination of μ_b^*, μ_s, or physical scenario results in a significant flux of marine debris from China to Aldabra. More likely is an explanation suggested by Duhec et al. (2015), that a large proportion of labelled items from Asia accumulating at beaches in Seychelles were thrown overboard or lost from shipping activities in the vicinity of Seychelles. Indeed, this is strongly supported by Figure 4(d), which shows that Aldabra is directly downstream of the extremely busy shipping lanes linking SE Asia to the Atlantic. This same explanation could account for the number of bottles found on Aldabra from Thailand and Singapore, both of which were more than an order of magnitude more abundant in the cleanup than our predictions based on trajectory analysis. Shipping lanes aside, another possibility is that some waste entering the ocean from countries such as Indonesia was manufactured abroad. This could be due to the export of goods for sale and/or the export of waste. Indonesia is a major waste importer, but the main export partners are in Europe and the Americas (Greenpeace East Asia, 2019), so this cannot account for the discrepancies in Table 2. We do not have data on the proportion of bottled drinks sold in Indonesia (or other identified source countries) which are foreign imports, but imports would have to account for almost all PET bottles sold in these countries to explain the discrepancies in Table 2. We therefore suggest that disposal at sea is the most likely explanation for the discrepancies we have found.

Disposal at sea cannot, however, explain the under-representation of bottles from Philippines amongst PET bottles found at Aldabra relative to our predictions. We suggest the most likely explanation is that the value for μ_b^* diagnosed from drifters based on a global dataset is inappropriate for the complex archipelagic coastline and bathymetry around Philippines, resulting in our analyses underestimating the beaching rate for debris of Philippine origin.

Alphonse (Seychelles)

Dunlop et al. (2020) carried out a short-term marine debris monitoring program in 2013 at Alphonse and attempted to identify the country of origin for plastic and glass bottles (and caps) with intact labels. Dunlop et al. (2020) found that 75% of labelled items originated from Southeast Asia (primarily Indonesia and Thailand, although two glass bottles were found from Philippines), with 13% originating from East Asia (mainly China). Our model predicts that 46.5% of Class C debris beaching at Alphonse should originate from Indonesia and 13.5% from Philippines so, as with Aldabra, there is general agreement that a large proportion of beaching debris of terrestrial origin at Alphonse originates from Southeast Asia. As with Aldabra, Dunlop et al. (2020) found significantly more bottles of Chinese origin than predicted by our analysis, supporting their conclusion that these bottles were likely lost at sea relatively close to Alphonse. One interesting discrepancy is that our trajectory analysis predicts 30.0% of Class C debris at Alphonse originated from India or Sri Lanka, whereas Dunlop et al. (2020) did not identify any bottles from either of these countries. A difference in transport time cannot explain this difference, as the mean transport time from India and Sri Lanka to Alphonse should be less than that for debris of Indonesian origin.

Outer Islands of Seychelles

Based on a sample of 189 labels found on four islands in Seychelles (Alphonse, Coëtivy, Astove, and Platte), The Ocean Project Seychelles (2019) found that 49% of labels originated from SE Asia and specifically noted that the most common countries of origin were Indonesia

(26.5%), Mauritius (12%), and Malaysia (10.2%). This is broadly in line with the findings of the other debris monitoring programmes in Seychelles, although one exception is the large proportion of debris originating from Mauritius. Mauritius sits just to the south of the bifurcation point of the Southern Equatorial Current as it splits into the North Madagascan Current and Southeast Madagascan Current (Voldsund et al., 2017) and, as a result, debris from Mauritius is unlikely to be transported towards Seychelles, even accounting for the effects of winds. Given that no other studies assessing sources of debris in Seychelles noted a large proportion of debris from Mauritius ($< 4\%$ at Alphonse (Duhec et al., 2015), and no mention at Aldabra (Burt et al., 2020)), it is possible that these items from Mauritius instead originated from nearby ships.

4. Conclusions and implications for conservation

Environmental conservation NGOs have been burdened with the task of cleaning up vast quantities of marine debris arriving on coastlines across Seychelles and other small island developing states. Observations have suggested that most of these states are not responsible for the bulk of debris accumulating on their shores, but limited quantitative data are available on sources, hindering management of the issue through source interventions and pursuing the 'polluter pays principle'. We have provided the first quantitative estimates for the sources of marine debris (both terrestrial and marine in origin) across Seychelles, as well as other remote islands in the western Indian Ocean.

Our analyses suggest that Seychelles is a hotspot for marine debris accumulation from around the Indian Ocean. We estimate that a large proportion of debris beaching at Seychelles has drifted from southeast Asia (principally Indonesia) and, in the case of the Inner Islands, south Asia (primarily India and Sri Lanka). Since debris drifting from sources such as Indonesia will have been at sea for at least six months, this also increases the risk of invasive species and pathogen introductions through rafting from the eastern and northern Indian Ocean. These results emphasise the scale of the challenge facing small island developing states such as Seychelles, and underlines the need for multilateral discussions around waste management. Smaller debris fragments may originate from East Africa (mainly Tanzania) and from within Seychelles itself, although these are unlikely to account for most beaching debris by mass, particularly for the Outer Islands of Seychelles. Our results suggest that Seychelles as a whole is at very high risk from debris that has been lost from ships transiting the Indian Ocean, and that most debris accumulating at Seychelles from Malaysia, Thailand and, in particular, China, is likely associated with these shipping corridors. This prediction could be used to initiate discussions with shipping companies to reduce these sources of marine pollution. We have also found that abandoned, lost or otherwise discarded fishing gear has a high probability of beaching within Seychelles, directly polluting island ecosystems. Beaching purse-seine fragments are likely associated with fishing activity around Seychelles, but longline fragments could feasibly drift from fisheries across the southern Indian Ocean. Greater enforcement by regional governments of MARPOL Annex V (Marine Environment Protection Committee, 2017), forbidding the discharge of fishing gear and other plastics at sea, would reduce these sources of pollution, particularly for Aldabra.

We have also found that there is likely to be significant predictability in marine debris accumulation rates across Seychelles, primarily from a strong seasonal cycle controlled by the monsoons. For classes of debris experiencing a significant push from the winds, our analysis suggests debris from terrestrial sources and fisheries are most likely to beach at Seychelles (but most significantly the Aldabra, Farquhar, and Alphonse Groups) during the northeast monsoon and subsequent intermonsoon. Beach clean-ups should ideally take place after peak beaching (i.e. May to June for much of Seychelles) to reduce the likelihood of beached plastics breaking down into smaller unmanageable fragments and impacting ecosystems. We have also proposed a mechanism by which ENSO and the IOD may modulate this seasonal cycle, and have presented some evidence to suggest that marine debris beaching rates at the more southerly island groups within Seychelles may be greater during and following positive IOD phases. These predictions may be helpful for practitioners deciding when to carry out beach cleanup operations.

There is reasonable agreement between our predictions, and the limited quantitative observations of marine debris that are available from across Seychelles. Key discrepancies with observations have also highlighted the importance of shipping lanes as a source of marine debris for remote western Indian Ocean islands. Nevertheless, it is important to remember that our trajectory analysis relies on a large number of poorly constrained parameters. There is an urgent need for further studies on the rate of marine macrodebris fragmentation, biofouling, and sinking. Despite the number of marine debris modelling studies incorporating windage into simulations and acknowledging the important role it plays in determining drift trajectories, there are limited publicly available estimates of appropriate windage coefficients for common classes of marine debris. Additionally, this windage coefficient will likely change with time, as debris loses buoyancy and/or fragments. Finally, considerable uncertainty remains in the input function of marine debris into the ocean. Nevertheless, a strength of this study is that our results can be easily recomputed for different combinations of sinking rate, beaching rate, and windage so, if improved constraints in the future demonstrate that our classification of debris (into our four classes A-D) is inappropriate, it will be straightforward to recompute results with the dataset and scripts provided in the Supplementary Data.

Acknowledgements

This work was funded by NERC grant NE/S007474/1, and used the ARCHER2 UK National Supercomputing Service (https://www.archer2.ac.uk) and JASMIN, the UK collaborative data analysis facility. Data analyses in this study made use of a wide range of python modules, most significantly OceanParcels (Lange and Sebille, 2017; Delandmeter and van Sebille, 2019), numpy (Harris et al., 2020), xarray (Hoyer and Hamman, 2017), scipy (Virtanen et al., 2020), cmasher (van der Velden, 2020), and matplotlib (Hunter, 2007). We are particularly grateful to all developers of OceanParcels, who have enormously improved the accessibility of Lagrangian particle tracking as a research tool. We thank Isla MacMillan for her advice on the manuscript, and rerunning analyses to compute the seasonality of dFADs between the Inner and Outer Islands of Seychelles. We thank Mirjam van der Mheen, Stuart Dunlop, and Lourens Meijer, for making raw data available from their studies upon request. We express our sincere thanks to the Compagnie Franaise du Thon Ocanique (CFTO), SAPMER and Via Océan for making their dFAD tracking data available, and to the Ob7, the pelagic ecosystem observatory of the IRD, for data management and preparation, and are grateful to L. Floch for data preparation. Finally, we thank all individuals who were involved in the Aldabra Cleanup Project, who have helped protect such an important and

special island and whose work inspired this research project.

Data Availability Statement

All data and scripts required to reproduce the figures in the main text are archived at the British Oceanographic Data Centre (link)[2], with the exception of dFAD deployment data due to a confidentiality agreement. Requests for access to dFAD deployment and tracking data should be addressed directly to the Ob7 pelagic ecosystem observatory (https://www.ob7.ird.fr/) using the following email address: adm-dblp@ird.fr.

References

Backeberg, B.C., Reason, C.J., 2010. A connection between the South Equatorial Current north of Madagascar and Mozambique Channel Eddies. Geophysical Research Letters 37, 1–6. doi:10.1029/2009GL041950.

Bergmann, M., Lutz, B., Tekman, M.B., Gutow, L., 2017. Citizen scientists reveal: Marine litter pollutes Arctic beaches and affects wild life. Marine Pollution Bulletin 125, 535–540. URL: https://doi.org/10.1016/j.marpolbul.2017.09.055, doi:10.1016/j.marpolbul.2017.09.055.

Bosi, S., Broström, G., Roquet, F., 2021. The Role of Stokes Drift in the Dispersal of North Atlantic Surface Marine Debris. Frontiers in Marine Science 8, 1–15. doi:10.3389/fmars.2021.697430.

[2]Note: these data are currently undergoing archival, which will be complete by the time this paper is published. This link is static, and will direct to the full dataset once archival is complete.

Bretherton, C.S., Widmann, M., Dymnikov, V.P., Wallace, J.M., Bladé, I., 1999. The effective number of spatial degrees of freedom of a time-varying field. Journal of Climate 12, 1990–2009. doi:10.1175/1520-0442(1999)012<1990:TENOSD>2.0.CO;2.

Burt, A.J., Raguain, J., Sanchez, C., Brice, J., Fleischer-Dogley, F., Goldberg, R., Talma, S., Syposz, M., Mahony, J., Letori, J., Quanz, C., Ramkalawan, S., Francourt, C., Capricieuse, I., Antao, A., Belle, K., Zillhardt, T., Moumou, J., Roseline, M., Bonne, J., Marie, R., Constance, E., Suleman, J., Turnbull, L.A., 2020. The costs of removing the unsanctioned import of marine plastic litter to small island states. Scientific Reports 10, 1–10. URL: https://doi.org/10.1038/s41598-020-71444-6, doi:10.1038/s41598-020-71444-6.

Cardoso, C., Caldeira, R.M., 2021. Modeling the Exposure of the Macaronesia Islands (NE Atlantic) to Marine Plastic Pollution. Frontiers in Marine Science 8. doi:10.3389/fmars.2021.653502.

Cerdeiro, D.A., Komaromi, A., Liu, Y., Saeed, M., 2020. World Seaborne Trade in Real Time : A Proof of Concept for Building AIS-based Nowcasts from Scratch. IMF Working Paper URL: https://www.imf.org/en/Publications/WP/Issues/2020/05/14/World-Seaborne-Trade-in-Real-Time-A-Proof-of-Concept-for-Building-AIS-based-Nowcasts-

Chassignet, E.P., Xu, X., Zavala-Romero, O., 2021. Tracking Marine Litter With a Global Ocean Model: Where Does It Go? Where Does It Come From? Frontiers in Marine Science 8, 1–15. doi:10.3389/fmars.2021.667591.

Cózar, A., Echevarría, F., González-Gordillo, J.I., Irigoien, X., Úbeda, B., Hernández-León, S., Palma, .T., Navarro, S., García-de Lomas, J., Ruiz, A., Fernández-de Puelles, M.L., Duarte, C.M., 2014. Plastic debris in the open ocean. Proceedings of the National Academy of Sciences of the United States of America 111, 10239–10244. doi:10.1073/pnas.1314705111.

Delandmeter, P., van Sebille, E., 2019. The Parcels v2.0 Lagrangian framework: new field interpolation schemes. Geoscientific Model Development Discussions , 1–24URL: https://doi.org/10.5194/gmd-2018-339, doi:10.5194/gmd-2018-339.

Domon, A., Izumiya, T., Ishibashi, K., 2012. STUDY ON THE DRAG COEFFICIENT RATIO OF DRIFTING OBJECTS DUE TO WIND AND WAVES AND PREDICTION OF LEEWAY TRAJECTORY. Journal of Japan Society of Civil Engineers, Ser. B3 (Ocean Engineering) 68, 1031–1036. URL: https://www.jstage.jst.go.jp/article/jscejoe/68/2/68_I_1031/_article/-char/ja/, doi:10.2208/jscejoe.68.I{_}1031.

Duhec, A.V., Jeanne, R.F., Maximenko, N., Hafner, J., 2015. Composition and potential origin of marine debris stranded in the Western Indian Ocean on remote Alphonse Island, Seychelles. Marine Pollution Bulletin 96, 76–86. doi:10.1016/j.marpolbul.2015.05.042.

van Duinen, B., Kaandorp, M.L., van Sebille, E., 2022. Identifying Marine Sources of Beached Plastics Through a Bayesian Framework: Application to Southwest Netherlands. Geophysical Research Letters 49, 1–9. doi:10.1029/2021GL097214.

Dunlop, S.W., Dunlop, B.J., Brown, M., 2020. Plastic pollution in paradise: Daily accumulation rates of marine litter on Cousine Island, Seychelles. Marine Pollution Bulletin 151, 110803. URL: https://doi.org/10.1016/j.marpolbul.2019.110803, doi:10.1016/j.marpolbul.2019.110803.

Fazey, F.M., Ryan, P.G., 2016. Biofouling on buoyant marine plastics: An experimental study into the effect of size on surface longevity. Environmental Pollution 210, 354–360. URL: http://dx.doi.org/10.1016/j.envpol.2016.01.026, doi:10.1016/j.envpol.2016.01.026.

Gall, S.C., Thompson, R.C., 2015. The impact of debris on marine life. Marine Pollution Bulletin 92, 170–179. URL: http://dx.doi.org/10.1016/j.marpolbul.2014.12.041, doi:10.1016/j.marpolbul.2014.12.041.

Greenpeace East Asia, 2019. Data From The Global Plastics Waste Trade 2016-2018 and The Offshore Impact of Chinas Foreign Waste Import Ban: An Analysis of Import-Export Data From The Top 21 Exporters and 21 Importers. Technical Report. URL: https://www.greenpeace.org/static/planet4-eastasia-stateless/2020/06/9858a41c-gpea-plastic-waste-trade-research-briefing-v2.pdf.

Harris, C.R., Millman, K.J., van der Walt, S.J., Gommers, R., Virtanen, P., Cournapeau, D., Wieser, E., Taylor, J., Berg, S., Smith, N.J., Kern, R., Picus, M., Hoyer, S., van Kerkwijk, M.H., Brett, M., Haldane, A., del Río, J.F., Wiebe, M., Peterson, P., Gérard-Marchant, P., Sheppard, K., Reddy, T., Weckesser, W., Abbasi, H., Gohlke, C., Oliphant, T.E., 2020. Array programming with NumPy. Nature 585, 357–362. URL: http://dx.doi.org/10.1038/s41586-020-2649-2, doi:10.1038/s41586-020-2649-2.

Hersbach, H., Bell, B., Berrisford, P., Hirahara, S., Horányi, A., Muñoz-Sabater, J., Nicolas, J., Peubey, C., Radu, R., Schepers, D., Simmons, A., Soci, C., Abdalla, S., Abellan, X., Balsamo, G., Bechtold, P., Biavati, G., Bidlot, J., Bonavita, M., De Chiara, G., Dahlgren, P., Dee, D., Diamantakis, M., Dragani, R., Flemming, J., Forbes, R., Fuentes, M., Geer, A., Haimberger, L., Healy, S., Hogan, R.J., Hólm, E., Janisková, M., Keeley, S., Laloyaux, P., Lopez, P., Lupu, C., Radnoti, G., de Rosnay, P., Rozum, I., Vamborg, F., Villaume, S., Thépaut, J.N., 2020. The ERA5 global reanalysis. Quarterly Journal of the Royal Meteorological Society 146, 1999–2049. doi:10.1002/qj.3803.

Hoyer, S., Hamman, J., 2017. xarray: N-D labeled Arrays and Datasets in Python. Journal of Open Research Software 5, 10. doi:10.5334/jors.148.

Hunter, J.D., 2007. Matplotlib: A 2D Graphics Environment. Computing in Science & Engineering 9, 90–95. URL: http://ieeexplore.ieee.org/document/4160265/, doi:10.1109/MCSE.2007.55.

Imzilen, T., 2021. Analyse et modélisation des trajectoires des dispositifs à concentration de poissons dérivants (DCP) dans les zones océaniques tropicales et estimation des risques associés à leur déploiement. Ph.D. thesis. Sorbonne Université.

Imzilen, T., Lett, C., Chassot, E., Kaplan, D.M., 2021. Spatial management can significantly reduce dFAD beachings in Indian and Atlantic Ocean tropical tuna purse seine fisheries. Biological Conservation 254, 108939. URL: https://doi.org/10.1016/j.biocon.2020.108939, doi:10.1016/j.biocon.2020.108939.

Imzilen, T., Lett, C., Chassot, E., Maufroy, A., Goujon, M., Kaplan, D.M., 2022. Recovery at sea of abandoned, lost or discarded drifting fish aggregating devices. Nature Sustainability 5. doi:10.1038/s41893-022-00883-y.

Jambeck, J.R., Geyer, R., Wilcox, C., Siegler, T.R., Perryman, M., Andrady, A., Narayan, R., Law, K.L., 2015. Plastic waste inputs from land into the ocean. Science 347, 768–771. URL: https://science.sciencemag.org/CONTENT/347/6223/768.abstracthttps://www.science.org/doi/10.1126/science.1260352, doi:10.1126/science.1260352.

Kaandorp, M.L., Dijkstra, H.A., Van Sebille, E., 2020. Closing the Mediterranean Marine Floating Plastic Mass Budget: Inverse Modeling of Sources and Sinks. Environmental Science and Technology 54, 11980–11989. doi:10.1021/acs.est.0c01984.

Kaplan, D.M., Chassot, E., Amandé, J.M., Dueri, S., Demarcq, H., Dagorn, L., Fonteneau, A., 2014. Spatial management of Indian Ocean tropical tuna fisheries: potential and perspectives. ICES Journal of Marine Science 71, 1728–1749. URL: https://academic.oup.com/icesjms/article/71/7/1728/665606, doi:10.1093/icesjms/fst233.

Koelmans, A.A., Kooi, M., Law, K.L., Van Sebille, E., 2017. All is not lost: Deriving a top-down mass budget of plastic at sea. Environmental Research Letters 12. doi:10.1088/1748-9326/aa9500.

Kroodsma, D.A., Mayorga, J., Hochberg, T., Miller, N.A., Boerder, K., Ferretti, F., Wilson, A., Bergman, B., White, T.D., Block, B.A., Woods, P., Sullivan, B., Costello, C., Worm, B., 2018. Tracking the global footprint of fisheries. Science 359, 904–908. URL: http://www.ncbi.nlm.nih.gov/pubmed/29472481, doi:10.1126/science.aao5646.

Kuczenski, B., Vargas Poulsen, C., Gilman, E.L., Musyl, M., Geyer, R., Wilson, J., 2022. Plastic gear loss estimates from remote observation of industrial fishing activity. Fish and Fisheries 23, 22–33. doi:10.1111/faf.12596.

Lange, M., Sebille, E.V., 2017. Parcels v0.9: Prototyping a Lagrangian ocean analysis framework for the petascale age. Geoscientific Model Development 10, 4175–4186. doi:10.5194/gmd-10-4175-2017.

Law-Chune, S., 2021. Global Ocean Waves Reanalysis. doi:https://doi.org/10.48670/moi-00022.

Lebreton, L., Andrady, A., 2019. Future scenarios of global plastic waste generation and disposal. Palgrave Communications 5, 1–11. URL: http://dx.doi.org/10.1057/s41599-018-0212-7, doi:10.1057/s41599-018-0212-7.

Lebreton, L., Egger, M., Slat, B., 2019. A global mass budget for positively buoyant macroplastic debris in the ocean. Scientific Reports 9, 1–10. doi:10.1038/s41598-019-49413-5.

Lebreton, L., Slat, B., Ferrari, F., Sainte-Rose, B., Aitken, J., Marthouse, R., Hajbane, S., Cunsolo, S., Schwarz, A., Levivier, A., Noble, K., Debeljak, P., Maral, H., Schoeneich-Argent, R., Brambini, R., Reisser, J., 2018. Evidence that the Great Pacific Garbage Patch is rapidly accumulating plastic. Scientific Reports 8, 1–15. URL: http://dx.doi.org/10.1038/s41598-018-22939-w, doi:10.1038/s41598-018-22939-w.

Lellouche, J.M., Greiner, E., Bourdallé Badie, R., Garric, G., Melet, A., Drévillon, M., Bricaud, C., Hamon, M., Le Galloudec, O., Regnier, C., Candela, T., Testut, C.E., Gasparin, F., Ruggiero, G., Benkiran, M., Drillet, Y., Le Traon, P.Y., 2021. The Copernicus Global 1/12° Oceanic and Sea Ice GLORYS12 Reanalysis. Frontiers in Earth Science 9, 1–27. doi:10.3389/feart.2021.698876.

Liubartseva, S., Coppini, G., Lecci, R., Clementi, E., 2018. Tracking plastics in the Mediterranean: 2D Lagrangian model. Marine Pollution Bulletin 129, 151–162. doi:10.1016/j.marpolbul.2018.02.019.

Macmillan, I., Attrill, M.J., Imzilen, T., Lett, C., Walmsley, S., Chu, C., Kaplan, D.M., 2022. Spatio-temporal variability in drifting Fish Aggregating Device (dFAD) beaching events in the Seychelles Archipelago. ICES Journal of Marine Science 0, 1–14. doi:10.1093/icesjms/fsac091.

Marine Environment Protection Committee, 2017. Resolution MECP. 295(71): 2017 Guidelines for the Implementation of Marpol Annex V. URL: http://www.imo.org/en/OurWork/Environment/PollutionPrevention/Garbage/Documents/MEPC.295(71).pdf.

Martinez-Ribes, L., Basterretxea, G., Palmer, M., Tintoré, J., 2007. Origin and abundance of beach debris in the Balearic Islands. Scientia Marina 71, 305–314. URL: http://scientiamarina.revistas.csic.es/index.php/scientiamarina/article/view/10/10, doi:10.3989/scimar.2007.71n2305.

Maximenko, N., Hafner, J., Kamachi, M., MacFadyen, A., 2018. Numerical simulations of debris drift from the Great Japan Tsunami of 2011 and their verification with observational reports. Marine Pollution Bulletin 132, 5–25. URL: https://doi.org/10.1016/j.marpolbul.2018.03.056, doi:10.1016/j.marpolbul.2018.03.056.

Meijer, L.J., van Emmerik, T., van der Ent, R., Schmidt, C., Lebreton, L., 2021. More than 1000 rivers account for 80% of global riverine plastic emissions into the ocean. Science Advances 7, 1–14. doi:10.1126/sciadv.aaz5803.

van der Mheen, M., van Sebille, E., Pattiaratchi, C., 2020. Beaching patterns of plastic debris along the Indian Ocean rim. Ocean Science Discussions , 1–31doi:10.5194/os-2020-50.

Mihai, F.C., Gündoğdu, S., Khan, F.R., Olivelli, A., Markley, L.A., van Emmerik, T., 2022. Plastic pollution in marine and freshwater environments: abundance, sources, and mitigation, in: Emerging Contaminants in the Environment. Elsevier, pp. 241–274. URL: https://linkinghub.elsevier.com/retrieve/pii/B9780323851602000160, doi:10.1016/B978-0-323-85160-2.00016-0.

Nelms, S.E., Duncan, E.M., Broderick, A.C., Galloway, T.S., Godfrey, M.H., Hamann, M., Lindeque, P.K., Godley, B.J., 2016. Plastic and marine turtles: A review and call for research. ICES Journal of Marine Science 73, 165–181. doi:10.1093/icesjms/fsv165.

Newman, S., Watkins, E., Farmer, A., Brink, P.t., Schweitzer, J.P., 2015. The Economics of Marine Litter, in: Marine Anthropogenic Litter. Springer International Publishing, Cham, pp. 367–394. URL: http://link.springer.com/10.1007/978-3-319-16510-3_14, doi:10.1007/978-3-319-16510-3{_}14.

OECD, 1975. The Polluter Pays Principle. Technical Report. Paris. URL: https://www.oecd-ilibrary.org/environment/the-polluter-pays-principle_9789264044845-en, doi:10.1787/9789264044845-en.

Okubo, A., 1971. Oceanic diffusion diagrams. Deep-Sea Research and Oceanographic Abstracts 18, 789–802. doi:10.1016/0011-7471(71)90046-5.

Onink, V., Jongedijk, C.E., Hoffman, M.J., van Sebille, E., Laufkötter, C., 2021. Global simulations of marine plastic transport show plastic trapping in coastal zones. Environmental Research Letters 16, 064053. doi:10.1088/1748-9326/abecbd.

Richardson, A., 2022. IOTC catch-effort assessment and AIS usage by flag-states in the Western Indian Ocean, 2016-2020. Technical Report. OceanMind. URL: https://www.bluemarinefoundation.com/2022/05/20/evidence-of-unauthorised-fishing-by-eu-vessels-in-indian-ocean-coastal-states-waters/

Schott, F.A., Xie, S.P., McCreary, J.P., 2009. Indian ocean circulation and climate variability. Reviews of Geophysics 47, 1–46. doi:10.1029/2007RG000245.

van Sebille, E., Aliani, S., Law, K.L., Maximenko, N., Alsina, J., Bagaev, A., Bergmann, M., Chapron, B., Chubarenko, I., Cózar, A., Delandmeter, P., Egger, M., Fox-Kemper, B., Garaba, S.P., Goddijn-Murphy, L., Hardesty, D., Hoffman, M.J., Isobe, A., Jongedijk, C., Kaandorp, M., Khatmullina, L., Koelmans, A.A., Kukulka, T., Laufkötter, C., Lebreton, L., Lobelle, D., Maes, C., Martinez-Vicente, V., Morales Maqueda, M.A., Poulain-Zarcos, M., Rodriguez, E., Ryan, P.G., Shanks, A., Shim, W.J., Suaria, G., Thiel, M., van den Bremer, T., Wichmann, D., 2020. The physical oceanography of the transport of floating marine debris. Environmental Research Letters doi:10.1088/1748-9326/ab6d7d.

Seo, S., Park, Y.G., 2020. Destination of floating plastic debris released from ten major rivers around the Korean Peninsula. Environment International 138, 105655. URL: https://doi.org/10.1016/j.envint.2020.105655, doi:10.1016/j.envint.2020.105655.

Siegel, D.A., Mitarai, S., Costello, C.J., Gaines, S.D., Kendall, B.E., Warner, R.R., Winters, K.B., 2008. The stochastic nature of larval connectivity among nearshore marine populations. Proceedings of the National Academy of Sciences 105, 8974–8979. doi:10.1073/pnas.0802544105.

Smagorinsky, J., 1963. GENERAL CIRCULATION EXPERIMENTS WITH THE PRIMITIVE EQUATIONS. Monthly Weather Review 91, 99–164. URL: http://journals.ametsoc.org/doi/10.1175/1520-0493(1963)091%3C0099:GCEWTP%3E2.3.CO;2, doi:10.1175/1520-0493(1963)091<0099:GCEWTP>2.3.CO;2.

Stelfox, M., Lett, C., Reid, G., Souch, G., Sweet, M., 2020. Minimum drift times infer trajectories of ghost nets found in the Maldives. Marine Pollution Bulletin 154, 111037. URL: https://doi.org/10.1016/j.marpolbul.2020.111037, doi:10.1016/j.marpolbul.2020.111037.

The Ocean Project Seychelles, 2019. Preliminary report on the abundance , composition and potential origin of marine litter stranded on eight main outer islands/atolls of Seychelles observed during the Seychelles Outer Islands Clean-Up organised by the Islands Development Company. Technical Report June.

Thompson, R.C., Moore, C.J., Saal, F.S., Swan, S.H., 2009. Plastics, the environment and human health: Current consensus and future trends. Philosophical Transactions of the Royal Society B: Biological Sciences 364, 2153–2166. doi:10.1098/rstb.2009.0053.

Turrell, W.R., 2020. Estimating a regional budget of marine plastic litter in order to advise on marine management measures. Marine Pollution Bulletin 150, 110725. URL: https://doi.org/10.1016/j.marpolbul.2019.110725, doi:10.1016/j.marpolbul.2019.110725.

van der Velden, E., 2020. CMasher: Scientific colormaps for making accessible, informative and 'cmashing' plots. Journal of Open Source Software 5, 2004. doi:10.21105/joss.02004.

Virtanen, P., Gommers, R., Oliphant, T.E., Haberland, M., Reddy, T., Cournapeau, D., Burovski, E., Peterson, P., Weckesser, W., Bright, J., van der Walt, S.J., Brett, M., Wilson, J., Millman, K.J., Mayorov, N., Nelson, A.R., Jones, E., Kern, R., Larson, E., Carey, C.J., Polat, ., Feng, Y., Moore, E.W., VanderPlas, J., Laxalde, D., Perktold, J., Cimrman, R., Henriksen, I., Quintero, E.A., Harris, C.R., Archibald, A.M., Ribeiro, A.H., Pedregosa, F., van Mulbregt, P., Vijaykumar, A., Bardelli, A.P., Rothberg, A., Hilboll, A., Kloeckner, A., Scopatz, A., Lee, A., Rokem, A., Woods, C.N., Fulton, C., Masson, C., Häggström, C., Fitzgerald, C., Nicholson, D.A., Hagen, D.R., Pasechnik, D.V., Olivetti, E., Martin, E., Wieser, E., Silva, F., Lenders, F., Wilhelm, F., Young, G., Price, G.A., Ingold, G.L., Allen, G.E., Lee, G.R., Audren, H., Probst, I., Dietrich, J.P., Silterra, J., Webber, J.T., Slavič, J., Nothman, J., Buchner, J., Kulick, J., Schönberger, J.L., de Miranda Cardoso, J.V., Reimer, J., Harrington, J., Rodríguez, J.L.C., Nunez-Iglesias, J., Kuczynski, J., Tritz, K., Thoma, M., Newville, M., Kümmerer, M., Bolingbroke, M., Tartre, M., Pak, M., Smith, N.J., Nowaczyk, N., Shebanov, N., Pavlyk, O., Brodtkorb, P.A., Lee, P., McGibbon, R.T., Feldbauer, R., Lewis, S., Tygier, S., Sievert, S., Vigna, S., Peterson, S., More, S., Pudlik, T., Oshima, T., Pingel, T.J., Robitaille, T.P., Spura, T., Jones, T.R., Cera, T., Leslie, T., Zito, T., Krauss, T., Upadhyay, U., Halchenko, Y.O., Vázquez-Baeza, Y., 2020. SciPy 1.0: fundamental algorithms for scientific computing in Python. Nature Methods 17, 261–272. doi:10.1038/s41592-019-0686-2.

Voldsund, A., Aguiar-González, B., Gammelsrød, T., Krakstad, J.O., Ullgren, J., 2017.

Observations of the east Madagascar current system: Dynamics and volume transports. Journal of Marine Research 75, 531–555. doi:10.1357/002224017821836725.

Werner, S., Budziak, A., Van Franeker, J., Galgani, F., Hanke, G., Maes, T., Matiddi, M., Nilsson, P., Oosterbaan, L., Priestland, E., Thompson, R., Veiga, J., Vlachogianni, T., 2016. Harm caused by Marine Litter. Technical Report March 2017. European Commission. Luxembourg. URL: http://publications.jrc.ec.europa.eu/repository/bitstream/JRC104308/lbna28317enn.pdf, doi:10.2788/19937.

Woodall, L.C., Sanchez-Vidal, A., Canals, M., Paterson, G.L., Coppock, R., Sleight, V., Calafat, A., Rogers, A.D., Narayanaswamy, B.E., Thompson, R.C., 2014. The deep sea is a major sink for microplastic debris. Royal Society Open Science 1. doi:10.1098/rsos.140317.

Yu, W., Xiang, B., Liu, L., Liu, N., 2005. Understanding the origins of interannual thermocline variations in the tropical Indian Ocean. Geophysical Research Letters 32, 1–4. doi:10.1029/2005GL024327.

Zhang, Z., Wu, H., Peng, G., Xu, P., Li, D., 2020. Coastal ocean dynamics reduce the export of microplastics to the open ocean. Science of the Total Environment 713, 136634. URL: https://doi.org/10.1016/j.scitotenv.2020.136634, doi:10.1016/j.scitotenv.2020.136634.